

Direct evidence of CRISPR-Cas9-mediated mitochondrial genome editing

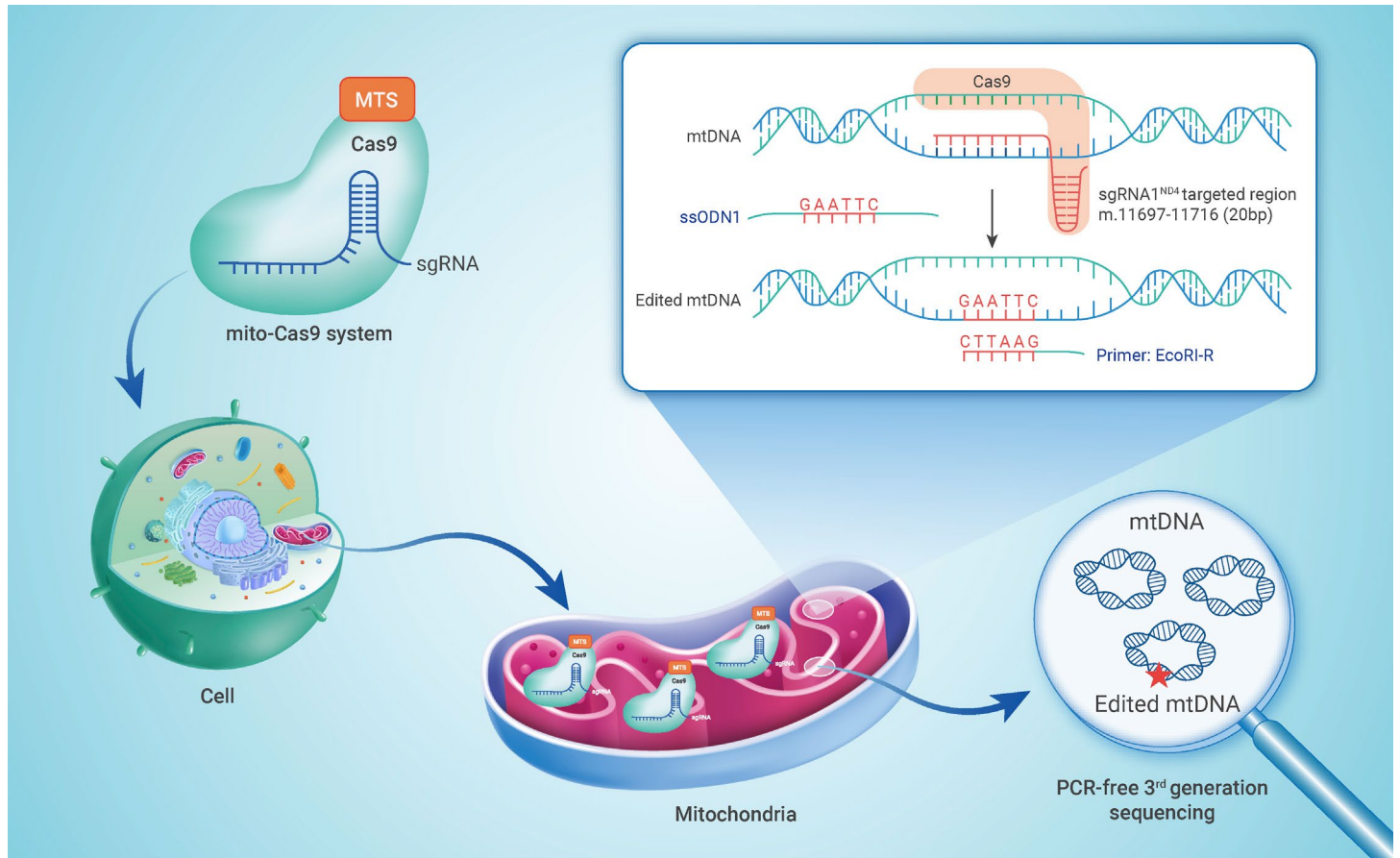
Rui Bi,^{1,2,3,10,*} Yu Li,^{1,2,10} Min Xu,^{1,2,10} Quanzhen Zheng,¹ Deng-Feng Zhang,^{1,2} Xiao Li,^{1,2} Guolan Ma,⁴ Bolin Xiang,^{1,2} Xiaojia Zhu,^{1,2} Hui Zhao,^{5,6} Xingxu Huang,⁷ Ping Zheng,^{2,6,8,9} and Yong-Gang Yao^{1,2,3,6,*}

*Correspondence: birui@mail.kiz.ac.cn (R.B.); yaoyg@mail.kiz.ac.cn (Y.-G.Y.)

Received: January 4, 2022; Accepted: September 23, 2022; Published Online: September 27, 2022; <https://doi.org/10.1016/j.xinn.2022.100329>

© 2022 The Author(s). This is an open access article under the CC BY-NC-ND license (<http://creativecommons.org/licenses/by-nc-nd/4.0/>).

GRAPHICAL ABSTRACT



PUBLIC SUMMARY

- We designed a mitochondria-targeted Cas9 system for successful mtDNA editing.
- Cas9-edited mtDNA was confirmed by the PCR-free third-generation sequencing.
- RAD51 agonist RS-1 significantly enhanced mtDNA knockin efficiency.

Direct evidence of CRISPR-Cas9-mediated mitochondrial genome editing

Rui Bi,^{1,2,3,10,*} Yu Li,^{1,2,10} Min Xu,^{1,2,10} Quanzhen Zheng,¹ Deng-Feng Zhang,^{1,2} Xiao Li,^{1,2} Guolan Ma,⁴ Bolin Xiang,^{1,2} Xiaojia Zhu,^{1,2} Hui Zhao,^{5,6} Xingxu Huang,⁷ Ping Zheng,^{2,6,8,9} and Yong-Gang Yao^{1,2,3,6,*}

¹Key Laboratory of Animal Models and Human Disease Mechanisms of the Chinese Academy of Sciences & Yunnan Province, Kunming Institute of Zoology, Chinese Academy of Sciences, Kunming, Yunnan 650204, China

²Kunming College of Life Science, University of Chinese Academy of Sciences, Kunming, Yunnan 650204, China

³Center for Excellence in Brain Science and Intelligence Technology, Chinese Academy of Sciences, Shanghai 200031, China

⁴Kunming Biological Diversity Regional Center of Large Apparatus and Equipments, Public Technology Service Center, Kunming Institute of Zoology, Chinese Academy of Sciences, Kunming, Yunnan 650204, China

⁵Key Laboratory for Regenerative Medicine, Ministry of Education, School of Biomedical Sciences, Faculty of Medicine, Chinese University of Hong Kong, and Hong Kong Branch of CAS Center for Excellence in Animal Evolution and Genetics, Hong Kong SAR, China

⁶KIZ/CUHK Joint Laboratory of Bioresources and Molecular Research in Common Diseases, Kunming Institute of Zoology, Chinese Academy of Sciences, Kunming, Yunnan 650204, China

⁷School of Life Science and Technology, ShanghaiTech University, Shanghai 201210, China

⁸State Key Laboratory of Genetic Resources and Evolution, and Yunnan Key Laboratory of Animal Reproduction, Kunming Institute of Zoology, Chinese Academy of Sciences, Kunming, Yunnan 650204, China

⁹Center for Excellence in Animal Evolution and Genetics, Chinese Academy of Sciences, Kunming, Yunnan 650204, China

¹⁰These authors contributed equally

*Correspondence: birui@mail.kiz.ac.cn (R.B.); yaoyg@mail.kiz.ac.cn (Y.-G.Y.)

Received: January 4, 2022; Accepted: September 23, 2022; Published Online: September 27, 2022; <https://doi.org/10.1016/j.xinn.2022.100329>

© 2022 The Author(s). This is an open access article under the CC BY-NC-ND license (<http://creativecommons.org/licenses/by-nc-nd/4.0/>).

Citation: Bi R., Li Y., Xu M., et al., (2022). Direct evidence of CRISPR-Cas9-mediated mitochondrial genome editing. *The Innovation* **3**(6), 100329.

Pathogenic mitochondrial DNA (mtDNA) mutations can cause a variety of human diseases. The recent development of genome-editing technologies to manipulate mtDNA, such as mitochondria-targeted DNA nucleases and base editors, offer a promising way for curing mitochondrial diseases caused by mtDNA mutations. The CRISPR-Cas9 system is a widely used tool for genome editing; however, its application in mtDNA editing is still under debate. In this study, we developed a mito-Cas9 system by adding the mitochondria-targeted sequences and 3' untranslated region of nuclear-encoded mitochondrial genes upstream and downstream of the Cas9 gene, respectively. We confirmed that the mito-Cas9 system was transported into mitochondria and enabled knockin of exogenous single-stranded DNA oligonucleotides (ssODNs) into mtDNA based on proteinase and DNase protection assays. Successful knockin of exogenous ssODNs into mtDNA was further validated using polymerase chain reaction-free third-generation sequencing technology. We also demonstrated that RS-1, an agonist of RAD51, significantly increased knockin efficiency of the mito-Cas9 system. Collectively, we provide direct evidence that mtDNA can be edited using the CRISPR-Cas9 system. The mito-Cas9 system could be optimized as a promising approach for the treatment of mitochondrial diseases caused by pathogenic mtDNA mutations, especially those with homoplasmic mtDNA mutations.

INTRODUCTION

Mitochondria play essential roles in cell metabolism, energy production, apoptosis, calcium homeostasis, and immunity.^{1,2} Mammalian mitochondria are double-membrane organelles with their own genome (mitochondrial DNA [mtDNA]). Human mtDNA is a double-stranded circular molecule composed of 16,569 base pairs (bp), containing 37 genes encoding 13 respiratory chain subunits, 22 transfer RNAs, and 2 ribosomal RNAs (rRNAs).³ Mitochondrial dysfunction resulting from mtDNA mutations can cause a variety of human diseases.^{1,2} There are 100–100,000 copies of the mtDNA genome in a cell, depending on the cell type.^{3,4} Mutant and wild-type mtDNA can co-exist in one cell, known as heteroplasmy.⁵ The level of heteroplasmy in pathogenic mtDNA mutations can affect disease onset and clinical phenotype, with a general threshold of 60%–95% of mutant mtDNA causing biochemical and clinical defects.^{6–8}

Currently, curing mitochondrial diseases remains a daunting task. Gene therapy through allotopic expression of mitochondrial genes shows promise for the treatment of Leber hereditary optic neuropathy⁹ caused by mtDNA mutations.¹⁰ Another approach is mitochondrial replacement therapy, which transfers the patient's spindle, pronuclear, or polar body genome into healthy enucleated donor oocytes or embryos to circumvent mother-to-child mtDNA disease transmission.^{4,11,12} With the rapid development of genome-editing technology, several approaches for manipulating mtDNA *in vitro* and *in vivo* have been established in

recent years,^{13–23} which exploit the rapid degradation of damaged mtDNA with double-strand breaks (DSBs) via mtDNA replisome components.^{24,25} For instance, mitochondria-targeted DNA nucleases specific to mutant mtDNA, including mitochondrial endonucleases,^{14,16,20} mitochondrial transcription activator-like effector nucleases (mito-TALENs),^{18–20,22} mitochondrial zinc-finger nucleases (mito-ZFNs),^{13,15,17,21} and mitochondrial meganucleases,²³ can specifically induce DSBs and promote the degradation of mutant mtDNA. These approaches can effectively shift the heteroplasmic level of mutant mtDNA^{13–23} but are limited by the unavailability of homoplasmic pathogenic mtDNA mutations. A bacterial cytidine deaminase fused with mito-TALEN (DdCBE) was recently established to induce base editing for C > T transition in mtDNA,²⁶ with successful application in mice, rats, zebrafish, plants, and human embryos.^{27–31} More recently, small-sized zinc-finger deaminases (ZFDs) were engineered for precise C > T base editing of nuclear and mitochondrial genes,³² offering several advantages in therapeutic application. The same research team also developed an A > G base editor for mtDNA (TALED, transcription activator-like effector-linked deaminases), providing a broader scope for mtDNA editing.³³ However, although base editors are promising tools for mtDNA editing, their substantial off-target effects on nuclear genes remain poorly resolved.^{34,35} Moreover, no current tools are able to induce or edit other types of mutations such as insertions, deletions, and transversions in mtDNA molecules.

The CRISPR-Cas9 system is a widely used tool for genome editing.³⁶ The core principle is to induce DSBs in the targeted genomic region, then complete genome editing via DSB repair pathways, including the non-homologous end joining (NHEJ), microhomology-mediated end joining (MMEJ), and homologous recombination (HR) pathways.³⁷ The CRISPR-Cas9 system is user friendly and flexible, and can circumvent the limitations of TALENs and ZFNs.³⁸ However, the suitability and efficiency of mtDNA editing by CRISPR-Cas9 remains controversial.³⁹ First, DSB repair is inefficient in mammalian mitochondria^{24,25} but is essential for successful editing by CRISPR-Cas9. Second, delivery of small-guide RNA (sgRNA) and Cas9 protein complexes into mitochondria is challenging. Several recent studies have attempted to manipulate mtDNA using the CRISPR-Cas9 system,^{40–45} which confirmed that the Cas9 protein can be transported into mitochondria, and that sgRNAs show mitochondrial localization.^{40,43} Most of these studies assessed successful manipulation of mtDNA mediated by CRISPR-Cas9 based on a decrease in mtDNA copy number^{40–43} and positive signals of allele-specific polymerase chain reaction (PCR) and/or PCR-based sequencing.^{42,44} Although these studies suggest the possibility of using CRISPR-Cas9 to manipulate mtDNA, PCR-based methods may be limited in their detection of edited mtDNA due to “template switching” or other technical artifacts.^{46–48} Furthermore, evidence showing successful mtDNA

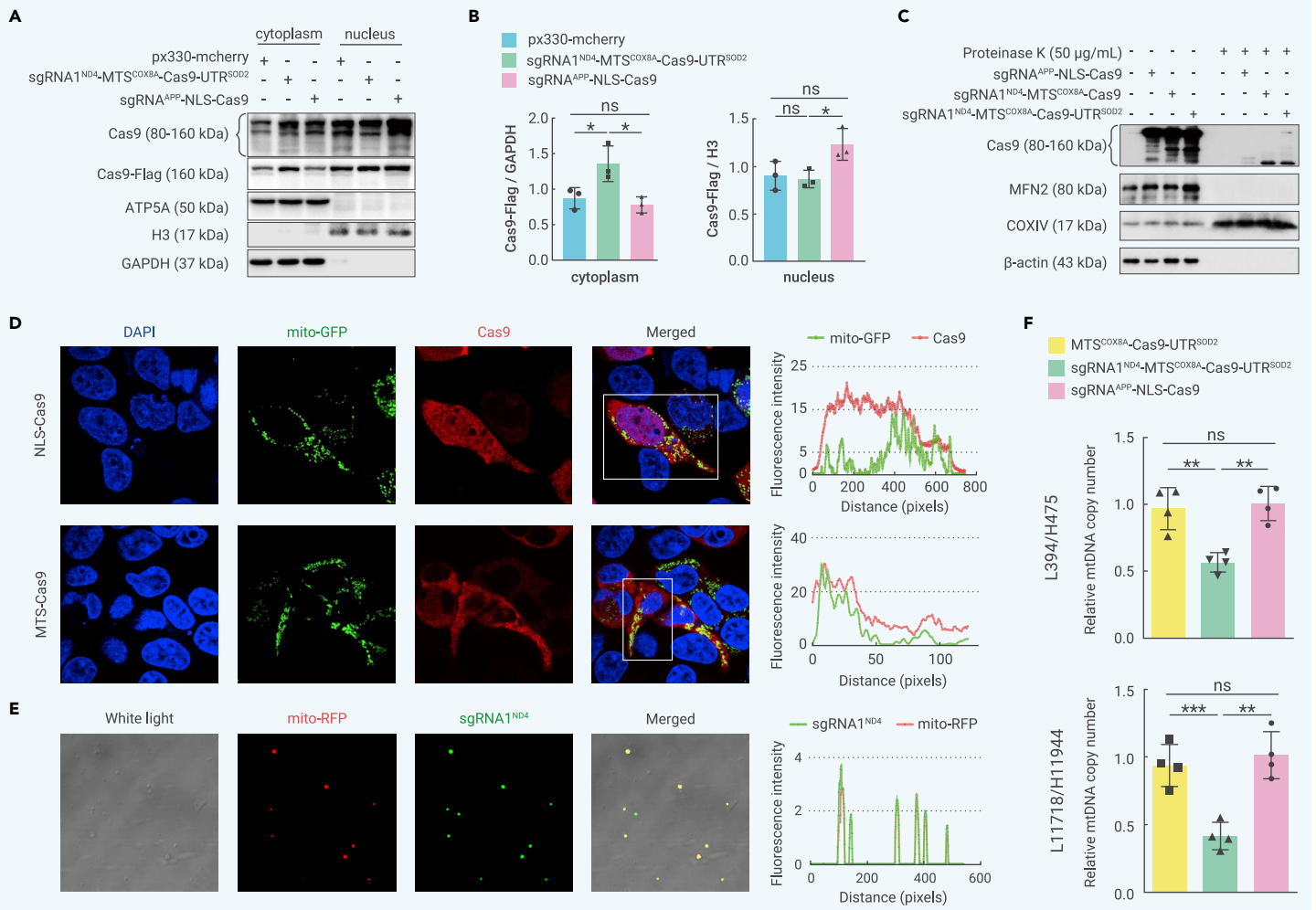


Figure 1. Mitochondrial localization of Cas9 protein and decreased mtDNA copy number. (A) Distribution of Cas9 protein in different cellular fractions. Nuclear and cytoplasmic fractions from HEK293T cells transfected with different Cas9 constructs were extracted for western blotting. Blot for H3 protein refers to nuclear fraction, whereas ATP5A and GAPDH refer to cytoplasmic fraction. Overexpression of Cas9 was determined using antibodies for Cas9 and Flag, respectively. (B) Quantification of the relative protein level of Cas9-Flag in (A). Levels of Cas9-Flag protein in cytoplasmic and nuclear fractions were normalized to GAPDH and H3, respectively. Bars represent mean \pm standard deviation (SD) of three independent tests. (C) Proteinase protection assay and western blot analysis showing successful expression and translocation of Cas9 into mitochondria. HEK293T cells were transfected with different mito-Cas9 constructs. Crude mitochondria were isolated at 48 h after transfection, and 20 μ g of crude mitochondrial fraction was treated with 50 μ g/mL proteinase K for 30 min on ice, followed by western blotting, with 10 μ g of crude mitochondrial fraction as a control. (D) Immunofluorescence assay showing mitochondrial localization of Cas9. HEK293T cells were co-transfected with mito-GFP vector (expressing mitochondrial-targeted green fluorescent protein) and Cas9 constructs (NLS-Cas9: construct sgRNA^{APP}-NLS-Cas9 with removal of mCherry; MTS-Cas9: construct sgRNA^{ND4}-MTS^{COX8A}-Cas9-UTR^{SOD2} with removal of mCherry). Cells were imaged at 488 nm (for mito-GFP) and 594 nm (for Cas9), respectively. Line graphs on right indicate fluorescence intensity in the rectangle in left images. (E) Mitochondrial localization of FAM-labeled sgRNA^{ND4}. Crude mitochondria were isolated from HEK293T cells co-transfected with FAM-labeled sgRNA^{ND4} and pDsRed2-mito vector (expressing mitochondria-targeted red fluorescent protein, mito-RFP) for 48 h. (F) Quantification of mtDNA copy number in HEK293T cells transfected with nuclear-targeted Cas9 vector (sgRNA^{APP}-NLS-Cas9), mitochondria-targeted Cas9 without sgRNA (MTS^{COX8A}-Cas9-UTR^{SOD2}), and mito-Cas9 construct (sgRNA^{ND4}-MTS^{COX8A}-Cas9-UTR^{SOD2}). Two pairs of primers, L394/H475 and L11718/H11944, were used for cross-validation, and mtDNA content was normalized to single-copy nuclear gene β -globin. Bars are mean \pm SD. ns, not significant; * p < 0.05, ** p < 0.01, *** p < 0.001; one-way analysis of variance (ANOVA) test adjusted by Tukey's multiple comparisons test.

editing by CRISPR-Cas9 remains inconclusive, which is why Gammage et al. have argued that the mitochondrial genome may not be "CRISPR-ized."³⁹

In this study, we constructed a mito-Cas9 system, and confirmed that the system enabled successful knockin of exogenous single-stranded DNA oligonucleotides (ssODNs) into mtDNA using PCR-free third-generation sequencing technology. Furthermore, overexpression or activation of RAD51 significantly increased the knockin efficiency of the mito-Cas9 system. These results provide direct evidence of successful CRISPR-Cas9-mediated mitochondrial genome editing.

RESULTS

Mito-Cas9 system targeted mitochondria and decreased mtDNA content

We established the mito-Cas9 system by replacing the nuclear localization sequence (NLS) at the N terminus of Cas9 in the px330-mCherry vector with the MTS of COX8A, and the NLS at the C terminus of Cas9 with the 3' untranslated region (UTR) of SOD2 (Figure S1). The MTSs and 3' UTR of the respective mitochondrial genes efficiently mediated the mitochondrial localization of mRNA.^{49,50} Small-guide RNA, sgRNA^{ND4} (Table S1), was designed to target m.11 697-11 716 in the *MT-ND4* gene, with a G added to the 5'-position of the 20-bp guide

sequence to obtain efficient U6 transcription of sgRNA and overall efficiency of the CRISPR-Cas9 system,^{37,51,52} and was cloned to create the mito-Cas9 construct sgRNA^{ND4}-MTS^{COX8A}-Cas9-UTR^{SOD2} (Figure S1). Previous studies have shown that unmodified sgRNAs can co-fractionate with mitochondria,^{40,42,43} therefore we did not further modify the sgRNAs. We constructed other mito-Cas9 constructs with sgRNA2^{ND4} and MTSs of mitochondrial genes COX10 and SOD2 using a similar strategy (Figure S1).

As expected, HEK293T cells transfected with the Cas9 construct containing the MTS of COX8A (sgRNA^{ND4}-MTS^{COX8A}-Cas9-UTR^{SOD2}) contained more Cas9 protein in the cytoplasmic components than cells transfected with the same amount of px330-mCherry vector or sgRNA^{APP}-NLS-Cas9 vector (Figures 1A and 1B). We performed protease protection assays and confirmed the successful translocation of the Cas9 protein into the mitochondria of cells transfected with the mito-Cas9 system, albeit with low efficiency (Figure 1C). As shown in Figure 1C, the Cas9 proteins showed multiple bands (around 80–160 kDa) in samples with or without proteinase K treatment. A small fraction of the Cas9 protein with MTSs, together with COXIV (positive control for mitochondrial inner membrane proteins), was protected from proteinase K digestion by the mitochondrial

membrane. In contrast, the cytoplasmic protein β -actin and mitochondrial outer membrane protein MFN2 (used as negative controls) were completely digested by proteinase K (Figure 1C). Unlike COXIV, which was completely localized in the mitochondria, Cas9 (with or without MTSSs) was partially localized in the mitochondria and its protein level decreased significantly upon protease K treatment. In the immunofluorescence assays, the Cas9 protein with MTSSs showed preferred co-localization with mitochondrial green fluorescent protein (Figure 1D). Notably, despite the lack of NLS or MTS, overexpression of the Cas9 protein was still observed in the nucleus and crude mitochondria (Figures 1A–1D). However, the reason for this Cas9 distribution pattern remains unknown.

We extracted mitochondria from HEK293T cells co-transfected with 6-carboxyfluorescein (FAM)-labeled sgRNA1^{ND4} (100 bp) and pDsRed2-mito vector (expressing mitochondria-targeted red fluorescent protein [mito-RFP]). We observed significant co-localization of FAM-labeled sgRNA1^{ND4} and mito-RFP (Figure 1E). We further used flow cytometry to quantify the proportion of labeled mitochondria in the total mitochondrial extract. FAM-labeled sgRNA1^{ND4} signals were detected in the mitochondria labeled with mito-RFP, albeit at a relatively low frequency (Figure S2A). We observed similar results using MitoTracker to label mitochondria (Figure S2B). These results suggest that Cas9 with MTSSs and sgRNA can be (partially) transported into mitochondria.

Within cells, mtDNA with DSBs is rapidly degraded,²⁴ therefore, a reduction in mtDNA copy number can be used as a marker for mtDNA manipulation.^{40–42} Consistent with previous studies,^{40–43} we observed a significant reduction in mtDNA copy number in HEK293T cells overexpressing the mito-Cas9 construct sgRNA1^{ND4}-MTS^{COX8A}-Cas9-UTR^{SOD2} compared with cells overexpressing nuclear-targeted Cas9 (sgRNA^{APP}-NLS-Cas9) or non-targeted controls (MTS^{COX8A}-Cas9-UTR^{SOD2}, mito-Cas9 without sgRNA) (Figure 1F). We further assessed the effect of the mito-Cas9 system on mitochondrial function. Cells transfected with mitochondria-targeted Cas9 showed significantly increased levels of reactive oxygen species (ROS) and significantly decreased levels of adenosine triphosphate compared with cells transfected with nuclear-targeted Cas9 or Cas9 without any targeting sequence (Figure S3A), indicating decreased mitochondrial function upon mito-Cas9 expression. To investigate whether the reduction in mtDNA copy number in mito-Cas9-transfected cells was caused by increased ROS, we determined the mtDNA copy number in cells treated with vitamin K3 (vitK3, reported to increase cellular ROS level⁵³) and melatonin (reported to decrease cellular ROS⁵⁴). Compared with the other groups, cells transfected with mito-Cas9 showed a significant decrease in mtDNA copy number, regardless of treatments (Figure S3C).

To investigate whether the mito-Cas9 construct with an alternative sgRNA targeting a different mtDNA region could still be applied for mtDNA editing, we used sgRNA2^{ND4} (Table S1) targeting the m.11 851–11 868 (20 nt) region in the *MT-ND4* gene. Consistently, upon overexpression of the sgRNA2^{ND4}-MTS^{COX8A}-Cas9-UTR^{SOD2} construct, the mtDNA copy number decreased significantly (Figure S4A). Thus, the mito-Cas9 system established here can successfully target mitochondria and induce a decrease in mtDNA copy number.

Mito-Cas9 system-mediated knockin of exogenous ssODNs into mtDNA through homology-directed repair

Increasing evidence has demonstrated the existence of MMEJ-mediated and HR-mediated DSB repair in mammalian mitochondria.^{55–58} Here, we investigated whether the mito-Cas9 system can mediate homology-directed repair in mtDNA. Based on previous observations that homologous arms longer than 40 bp can achieve high knockin efficiency,^{37,59} we designed a 96-bp ssODN1 donor template (Table S1) that contained 45-bp homologous arms (left arm: homologous to m.11 669–11 713; right arm: homologous to m.11 714–11 758) flanking a 6-bp insertion of the *EcoRI* site (GAATTC) (Figure 2A; Table S1). The ssODN1 donor template and Cas9 constructs were co-transfected into HEK293T cells for 48 h, after which homology-directed repair of mtDNA was analyzed using PCR and quantitative real-time PCR (qRT-PCR) with the *EcoRI* site-specific primer pair L11338/*EcoRI*-R (Figures 2A and 2B; Table S1). *EcoRI* site-specific PCR products were not detected in cells transfected with MTS^{COX8A}-Cas9-UTR^{SOD2} alone, but were detected in cells transfected with ssODN1 alone (Figures 2B and S5), which may be, in part, due to potential “template switching artifacts” between the ssODN1 template and mtDNA molecule.^{46–48} In contrast, cells transfected with a combination of sgRNA1^{ND4}-MTS^{COX8A}-Cas9-UTR^{SOD2} and ssODN1

showed significantly increased *EcoRI* site-specific PCR products compared with different controls (Figure 2B). We also constructed mito-dCas9 (dead Cas9) with a targeting sgRNA1^{ND4} as a control, in which the catalytic activity of the SpCas9 protein was abolished by introducing two mutations, p.D10A and p.H840A.^{60,61} The relative level of *EcoRI* site-specific PCR products of the mito-dCas9 system showed no significant differences compared with the controls transfected with ssODN1 alone or with ssODN1 + MTS^{COX8A}-Cas9-UTR^{SOD2} (no sgRNA) (Figure 2C). These findings indicated that Cas9 activity is essential for the mito-Cas9 system. To investigate whether the increase in *EcoRI* site-specific PCR products was caused by the potentially higher transfection efficiency/stability of ssODN1 with the mito-Cas9 system, we transfected HEK293T cells with FAM-labeled ssODN1 (which can be introduced into mitochondria after transfection, Figure S6A) and mCherry-tagged Cas9 vectors (with or without different target sequences). The proportion of fluorescently labeled cells was quantified by flow cytometry. We observed similar levels of labeled cells among the transfected cells (Figure S6B), indicating that ssODN1 exhibits a similar level of transfection efficiency in different ssODN1 and Cas9 vector combinations.

We next verified insertion of the “GAATTC” sequence in the sgRNA1^{ND4}-target site of mtDNA by direct sequencing of the *EcoRI* site-specific PCR product (Figure 2D). Furthermore, we found that the mito-Cas9 constructs with different MTSSs of mitochondrial genes (*COX8A*, *COX10*, or *SOD2*) exhibited similar knockin efficiencies of exogenous ssODNs (Figure 2E). To exclude the potential effects of “template switching artifacts” during PCR, we quantified the level of ssODN1 within the transfected cells at 48, 96, and 144 h after transfection. We found that the relative amount of the *EcoRI* site-specific PCR product in cells transfected with ssODN1 significantly diminished with time and was barely detected at 144 h (Figure S7). In contrast, cells transfected with ssODN1 and the mito-Cas9 system contained a significantly higher level of the *EcoRI* site-specific PCR product relative to cells transfected with ssODN1 alone at each time point (Figure S7). Of note, a reduction in the *EcoRI* site-specific PCR product was observed with time (Figure S7), which might be attributed to the higher proliferation rate of cells with wild-type mtDNA compared with cells with edited mtDNA.

To further exclude potential contamination from other sources of mtDNA (e.g., leakage of mtDNA fragments in cytosol from damaged mitochondria) or mtDNA-like fragments (e.g., nuclear mitochondrial pseudogenes in the nuclear genome⁶²) outside the mitochondria, which could potentially be recognized as a target by the mito-Cas9 system, we performed a DNase protection assay to validate the successful knockin of exogenous ssODNs into mtDNAs located within the mitochondria (Figure 2F). Upon DNase I treatment, no PCR product could be amplified for the nuclear *APP* gene (Figure 2F), whereas the mtDNA PCR product (amplified by primer pair L11338/H11944) and *EcoRI* site-specific PCR product were visible, indicating that exogenous ssODNs were inserted into mtDNA and were protected from DNase I digestion by the mitochondrial membrane (Figure 2F). Quantification of the *EcoRI* site-specific PCR products showed that the mito-Cas9 construct sgRNA1^{ND4}-MTS^{COX8A}-Cas9-UTR^{SOD2} significantly increased the knockin efficiency of ssODN1 in both crude mtDNA (DNase–) and purified mtDNA (DNase+) (Figure 2G). The *EcoRI* site-specific PCR product was also detected when the target and knockin sites were changed (Figures S4B–S4D). Compared with cells transfected with ssODN2 alone or with a combination of ssODN2 and MTS^{COX8A}-Cas9-UTR^{SOD2} (no sgRNA), cells transfected with a combination of sgRNA2^{ND4}-MTS^{COX8A}-Cas9-UTR^{SOD2} and ssODN2 showed a significant increase in *EcoRI* site-specific PCR product (Figure S4D), indicating that mito-Cas9 system-mediated knockin can be applied to any site suitable for CRISPR-Cas9 editing. These results demonstrate that the mito-Cas9 system can mediate knockin of exogenous ssODNs into mtDNA through the HR repair pathway.

Third-generation sequencing verified knockin of exogenous ssODNs into mtDNA through mito-Cas9 system

To exclude the possibility that the *EcoRI* site-specific PCR products were caused by PCR artifacts, such as template-switching artifacts^{46–48} between exogenous ssODNs and mtDNA, we performed PCR-free third-generation sequencing to verify the knockin of exogenous ssODNs into mtDNA (Figure 3A). The ssODN1 donor template and mito-Cas9 construct sgRNA1^{ND4}-MTS^{COX8A}-Cas9-UTR^{SOD2} were co-transfected into HEK293T cells for 48 h. Cells transfected with ssODN1 only or with a combination of ssODN1 and MTS^{COX8A}-Cas9-UTR^{SOD2} (no sgRNA) were considered as controls. *BamHI* digestion was used to linearize purified

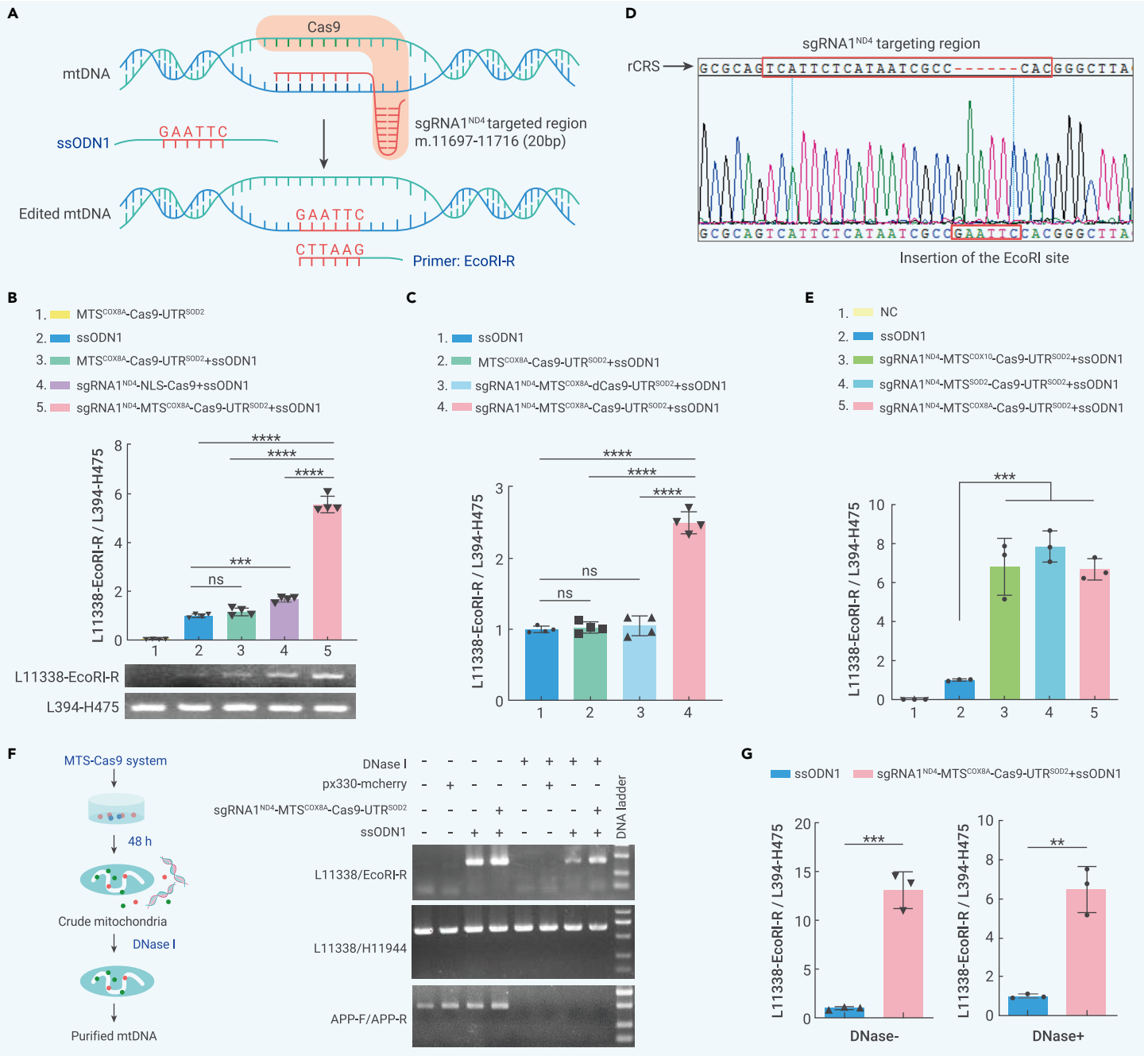


Figure 2. Mito-Cas9 system mediated efficient knockin of exogenous ssODNs into mtDNA (A) Design of mito-Cas9-mediated knockin system. (B) Quantification of knockin efficiency of mito-Cas9. (Upper) Results of qRT-PCR. HEK293T cells were transfected with or without a combination of Cas9 constructs and ssODN1. Content of mtDNA with successful knockin of *EcoRI* site (edited mtDNA, amplified by primer pair L11338/*EcoRI*-R (L11338-*EcoRI*-R)) was normalized to whole mtDNA (total mtDNA, amplified by primer pair L394/H475 (L394-H475)), using total genomic DNA as the template. (Below) Agarose gel image showing representative PCR product for each group of cells with different transfections. (C) Knockin efficiency of mito-Cas9 constructs with catalytically dead Cas9 (dCas9): sgRNA1^{ND4}-MTS^{COX8A}-dCas9-UTR^{SOD2}, expressing SpCas9 protein with mutations p.D10A and p.H840A. Knockin efficiency was quantified using the same qRT-PCR procedure as in (B), with total genomic DNA from respective transfected cells as the template. (D) Sequencing chromatogram of *EcoRI* site-specific PCR product. Targeting region of sgRNA1^{ND4} is marked with a box on the mtDNA revised Cambridge reference sequence (rCRS). (E) Knockin efficiency of different mito-Cas9 constructs with different MTSS. HEK293T cells were transfected with ssODN1 and mito-Cas9 construct fused with indicated MTSS of mitochondrial genes *COX8A*, *COX10*, or *SOD2*. Knockin efficiency was quantified using the same qRT-PCR procedure as in (B), with total genomic DNA from respective transfected cells as the template. (F) DNase I treatment assay confirmed the mitochondrial source of *EcoRI* site-specific PCR product amplified from edited mtDNA in mitochondria. Crude mitochondria were extracted from HEK293T cells transfected with sgRNA1^{ND4}-MTS^{COX8A}-Cas9-UTR^{SOD2} and ssODN1 for 48 h, then treated with DNase I at 37°C for 1 h. PCR amplifications for nuclear *APP* (amplified by primer pair APP-F/APP-R), total mtDNA (amplified by primer pair L11338/H11944), and edited mtDNA (amplified by primer pair L11338/*EcoRI*-R) were performed using mtDNA template extracted from mitochondria with or without DNase I treatment, respectively. (G) Quantification of knockin efficiency in mtDNAs from crude mitochondria treated with DNase I (DNase+) or without DNase I (DNase-). Bars are mean \pm SD. ns, not significant; **p < 0.01, ***p < 0.001, ****p < 0.0001; one-way ANOVA test adjusted by Tukey's multiple comparisons test for (B, C, and E); two-tailed Student's t test for (G).

mtDNA isolated from DNase I-treated mitochondria (Figure 3A). Total genomic DNA was completely digested by *Bam*HI and showed no clear bands on the gel, whereas successfully linearized mtDNA was evidenced by a single band of mtDNA after *Bam*HI digestion (Figure S8A). We also measured the efficiency of linearization by quantifying the mtDNA fragment flanking the *Bam*HI site using qRT-PCR with the primer pair L14054/H14573 (Table S1; linearized mtDNA could

not be amplified by L14054/H14573) and observed a significant decrease in the PCR product for purified mtDNA subjected to *Bam*HI compared with undigested samples (Figure S8B), indicating that mtDNA was thoroughly linearized. Direct sequencing of linearized mtDNA using PCR-free PacBio sequencing technology yielded a distinct sequence peak at ~16 kb (Figure 3B, left), indicating full-length capture and sequencing of the mtDNA genome. Reads Mapping using the

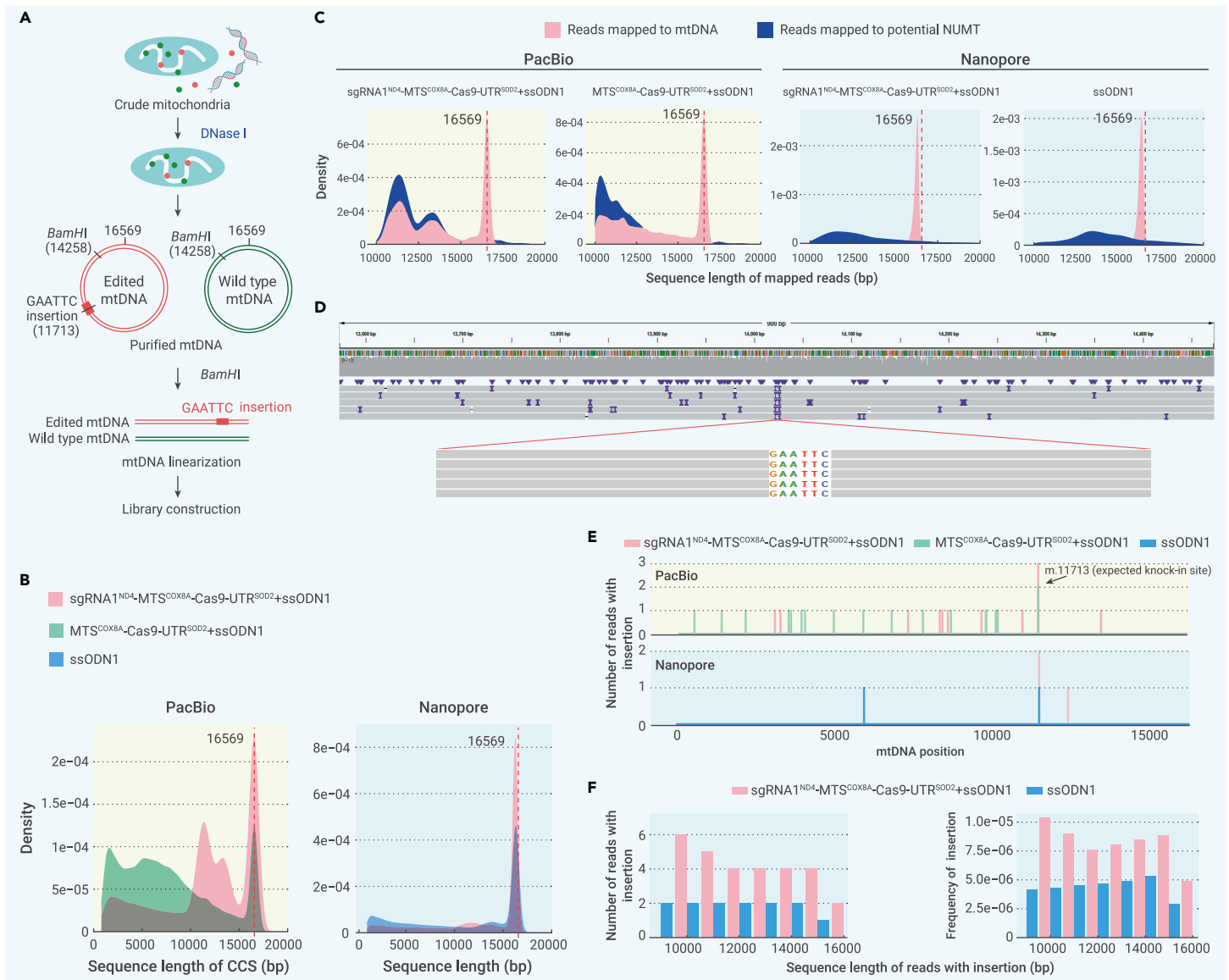


Figure 3. Third-generation sequencing identified mtDNA editing introduced by mito-Cas9 system (A) Flowchart of PCR-free third-generation sequencing of purified mtDNA. (B) Length distribution patterns of sequencing reads generated by PacBio (left) and Nanopore (right) sequencing. All reads were mapped to mtDNA. (C) Length distributions of sequencing reads mapped to mtDNA (pink) and potential NUMTs (blue). (D) Sequencing reads (>16 kb) showing successful knock-in of *EcoRI* site GAATTC at sgRNA1^{ND4}-targeted site. (E) Distribution of GAATTC insertion across the entire mtDNA genome based on sequencing reads >16 kb in length. (F) Counts (left) and frequencies (right) of mtDNA sequencing reads with targeted GAATTC insertion in all reads grouped by sequence length.

mtDNA reference sequence⁶³ and nuclear mitochondrial (NUMTs) reference sequences⁶⁴ showed that most reads mapped to NUMTs were <16 kb (Figure 3C, left). Therefore, we only used reads >16 kb in length, and with higher mapping percentage and concordance to mtDNA than to NUMTs, for the following analyses, thus reliably excluding the potential effects of NUMTs and other artifacts. We identified precise insertion of GAATTC at the sgRNA1^{ND4} target site in mtDNA reads from the entire mitochondrial genome (Figure 3D). Of note, a higher frequency of GAATTC insertion at the sgRNA1^{ND4} targeting site was observed for cells transfected with sgRNA1^{ND4}-MTS^{COX8A}-Cas9-UTR^{SOD2} + ssODN1 (3/11,484, 0.026%) than for control cells transfected with MTS^{COX8A}-Cas9-UTR^{SOD2} (no sgRNA) + ssODN1 (3/22,995, 0.0087%) (Figure 3E, top). In both samples, we observed randomly distributed GAATTC insertions across the mtDNA genome at extremely low frequencies (Figure 3E, top), which may be caused by potential errors in the third-generation sequencing technology.⁶⁵

To exclude the possibility that these targeted insertions were introduced by sequencing errors in PacBio Sequel II, we used another PCR-free sequencing method, Nanopore sequencing, to sequence mtDNAs extracted from cells transfected with sgRNA1^{ND4}-MTS^{COX8A}-Cas9-UTR^{SOD2} + ssODN1. In the captured reads across the entire mtDNA genome (peak near 16,569 bp; Figures 3B and 3C, right), we confirmed a higher rate of targeted GAATTC inser-

tion in cells transfected with sgRNA1^{ND4}-MTS^{COX8A}-Cas9-UTR^{SOD2} + ssODN1 (2/411,780) compared with cells transfected with ssODN1 alone (1/314,840) (Figure 3E, bottom). We observed several untargeted GAATTC insertions across the mtDNA genome in the PacBio data (Figure 3E, top), but these insertions were not replicated in the Nanopore sequencing data (Figure 3E, bottom), suggesting that most untargeted insertions were introduced by PacBio sequencing errors.⁶⁵ We further analyzed the number of reads with targeted insertions in the mtDNA sequencing data of different lengths. We identified a higher frequency of precise GAATTC insertions in mtDNA sequences larger than 10 kb at the sgRNA1^{ND4} target region in cells transfected with sgRNA1^{ND4}-MTS^{COX8A}-Cas9-UTR^{SOD2} + ssODN1 (n = 6) than in cells transfected with ssODN1 alone (n = 2) (Figure 3F). Overall, the total numbers of targeted insertions in the mtDNA sequences with different length cutoffs (from 10 to 16 kb) were consistently higher in cells transfected with the mito-Cas9 system than cells transfected with ssODN1 alone (Figure 3F). Therefore, the higher rate of targeted insertions in cells transfected with the mito-Cas9 system is unlikely to be due to random sequencing errors, but may be indicative of the editing capability of the mito-Cas9 system. The occurrence of targeted insertions in cells transfected with ssODN1 alone, even at a very low frequency, deserves further attention and focused study in the future, which may suggest an

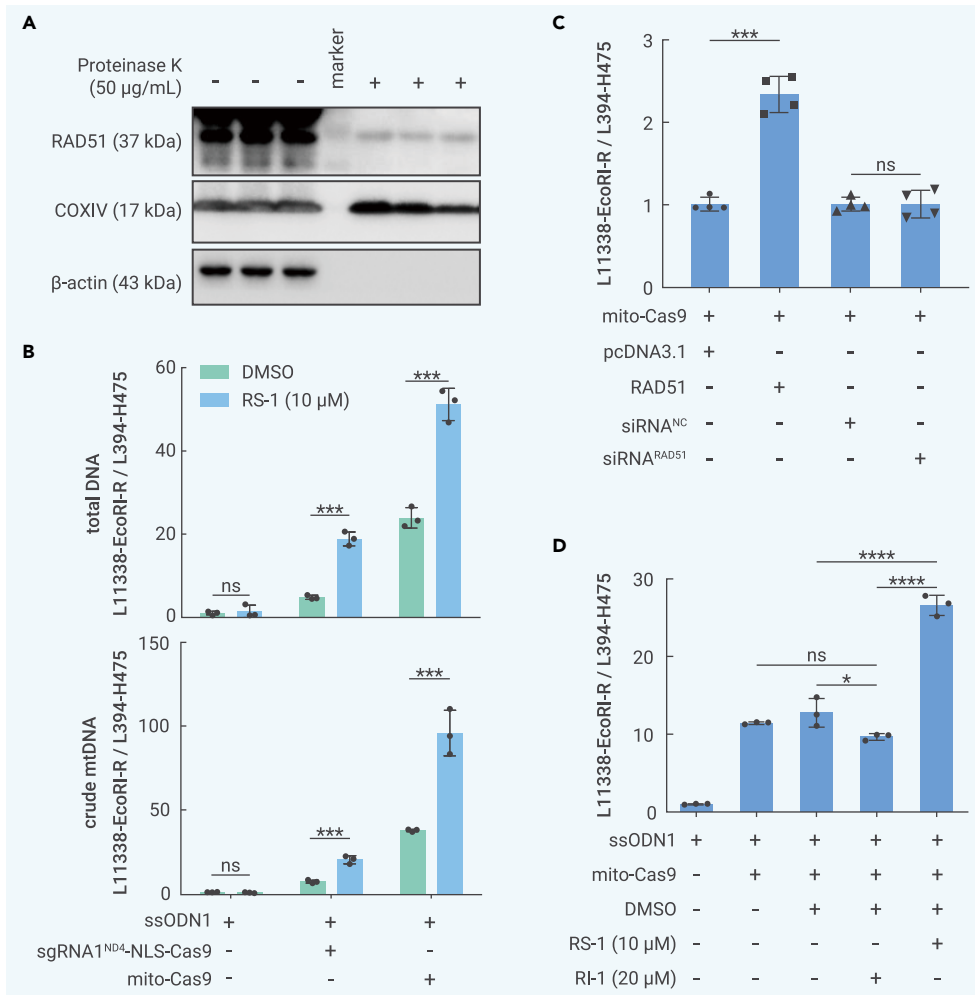


Figure 4. RAD51 was involved in mtDNA editing mediated by the mito-Cas9 system (A) RAD51 protein was detected in mitochondria from HEK293T cells treated with or without proteinase K. (B) RAD51 agonist RS-1 (10 µM) significantly increased knock-in efficiency of the mito-Cas9 system (sgRNA1^{ND4}-MTS^{COX8A}-Cas9-UTR^{SOD2} and ssODN1). Total genomic DNA (total DNA, upper) and mtDNA from crude mitochondria (crude mtDNA, lower) from transfected HEK293T cells with or without RS-1 treatment were used for quantification of edited mtDNA. (C) Overexpression of RAD51 protein significantly increased knockin efficiency of the mito-Cas9 system (sgRNA1^{ND4}-MTS^{COX8A}-Cas9-UTR^{SOD2} and ssODN1), but RAD51 knockdown did not affect knockin efficiency. HEK293T cells were co-transfected with expression vector of RAD51 and mito-Cas9 system for 48 h before harvest for qRT-PCR. (D) RAD51 inhibitor RI-1 (20 µM) decreased knockin efficiency of the mito-Cas9 system (sgRNA1^{ND4}-MTS^{COX8A}-Cas9-UTR^{SOD2} and ssODN1). Bars in (B)–(D) are mean ± SD. ns, not significant; *p < 0.05, ***p < 0.001, ****p < 0.0001; one-way ANOVA adjusted by Tukey's multiple comparisons test.

sgRNA1^{ND4}-NLS-Cas9 and ssODN1 compared with cells transfected with ssODN1 alone (Figure 4B). We speculated that this may be caused by a minimum level of sgRNA1^{ND4} guiding Cas9 and ssODN1 or penetration of Cas9 and ssODN1 into the mitochondria, similar to that observed for nuclear-imported Cas9 in the absence of NLS (Figure 1A).

We further quantified the knockin efficiency of the mito-Cas9 system using second-generation sequencing technology. Using a primer pair outside of ssODN1, we amplified a fragment flanking the knockin site (m.11 600–11 820) in crude and purified mtDNAs (Table 1; Figure S9E), respectively, then subjected the PCR products to second-generation sequencing. Knockin of ssODNs was identified in the sequencing reads

unexpected role of ssODN1 in the initiation of mtDNA replication in the absence of the mito-Cas9 system (Bi et al., unpublished data).

RAD51 activation enhanced mito-Cas9 system knockin efficiency

We further tested whether modulating those factors involved in genome stability maintenance and repair pathways could improve the knockin efficiency of the mito-Cas9 system. HR is essential for maintaining mitochondrial genome integrity.^{55,56,58} Key factors in the HR pathway, such as RAD51 and XRCC3, can be recruited to mitochondria and participate in mtDNA maintenance under DNA damage stress.^{58,66,67} We confirmed the presence of RAD51 in mitochondria using a proteinase protection assay (Figure 4A). As our mito-Cas9 system was based on HR-mediated effects, we hypothesized that enhancing RAD51 function would increase the knockin efficiency of ssODNs into mtDNA, as shown by the Cas9-mediated knockin efficiency for nuclear DNA.^{68–70} We treated HEK293T cells transfected with the mito-Cas9 construct sgRNA1^{ND4}-MTS^{COX8A}-Cas9-UTR^{SOD2} and/or ssODN1 with RAD51 agonist RS-1 (10 µM) for 42 h, then quantified the level of edited mtDNA (Figure 4B). Stimulation of RAD51 with RS-1 significantly increased the knockin efficiency of the mito-Cas9 system (Figure 4B), whereas RS-1 had no significant effect on cells transfected with ssODN1 alone (Figures 4B and S9A) or on the other three controls (mito-Cas9 without ssODN1, mito-Cas9 without sgRNA, and mito-Cas9 with sgRNA2^{ND4} targeting another region) (Figures 4B and S9A). Overexpression of the RAD51 protein resulted in a significant increase in the knockin efficiency of the mito-Cas9 system, similar to the treatment of the RAD51 agonist (Figures 4C and S9B). However, knockdown of RAD51 or inhibition of RAD51 by RI-1⁷¹ had no or a weak effect on the knockin efficiency of the mito-Cas9 system (Figures 4C, 4D, S9C, and S9D), suggesting a potential compensatory effect in cells with RAD51 knockdown or inhibition during the maintenance of genome stability. Interestingly, an increase in the *EcoRI* site-specific PCR product signal was observed in cells transfected with

(Table 1; Figure S9E). Consistent with the qRT-PCR results, in HEK293T cells transfected with the mito-Cas9 construct sgRNA1^{ND4}-MTS^{COX8A}-Cas9-UTR^{SOD2} and ssODN1, RS-1 treatment resulted in a nearly 5-fold increase in knockin efficiency in the crude mtDNA (0.14%) relative to that in cells without RS-1 treatment (0.03%; p < 2.2 × 10⁻¹⁶, Fisher's exact test) (Table 1). Knockin frequency further increased in the purified mtDNA (0.23%; p < 2.2 × 10⁻¹⁶, Fisher's exact test) (Table 1). Of note, the relative number of sequence reads with knockin was significantly lower (p < 2.2 × 10⁻¹⁶, Fisher's exact test) in cells transfected with ssODN1 alone than in cells transfected with mito-Cas9 constructs and ssODN1 (Table 1). Furthermore, no significant changes in knockin efficiency were observed in the ssODN1-transfected cells with or without RS-1 treatment, suggesting that sequence reads with GAATTC knockin in cells transfected with ssODNs alone were not HR mediated (Table 1).

Collectively, these results suggest that RAD51 is a key factor for the knockin of exogenous ssODNs into mtDNA. Small-molecule RS-1 increased knockin efficiency of the mito-Cas9 system through RAD51 activation, further supporting HR-mediated knockin of exogenous ssODNs into mtDNA. Although template switching artifacts or other potential factors may introduce some noise in regard to the interpretation of knockin frequency, this noise is unlikely to have contributed to the significant differences observed between groups.

Lack of evident off-target sites in nuclear genome by the mito-Cas9 system

We performed whole-genome sequencing (WGS) for genomic DNA isolated from HEK293T cells transfected with sgRNA1^{ND4}-MTS^{COX8A}-Cas9-UTR^{SOD2} + ssODN1 and sgRNA2^{ND4}-MTS^{COX8A}-Cas9-UTR^{SOD2} + ssODN2, respectively. Mean sequence depth for the two samples was about 34×. The nuclear genome was screened for potential off-target sites with "NGG" or "NAG" protospacer adjacent motif and with up to nine mismatches relative to sgRNA. No insertions or

Table 1. Frequency of reads with GAATTC knockin based on second-generation sequencing

Sample	Total no. of reads	No. of reads with GAATTC insertion	Knockin ratio
Crude mtDNA			
ssODN1	5,028,392	343	0.00006821
ssODN1 + RS-1	6,838,719	324	0.00004738
mito-Cas9 + ssODN1	5,367,579	1608	0.00029958
mito-Cas9 + ssODN1 + RS-1	6,208,098	8839	0.00142379
Purified mtDNA			
ssODN1 + RS-1	5,991,432	210	0.00003505
mito-Cas9 + ssODN1 + RS-1	4,992,779	11,714	0.00234619

Counts for sequencing reads with the GAATTC insertion in a short PCR fragment (region m.11 600–11 820 in mtDNA) flanking the knockin site. Crude mtDNA and purified mtDNA were used as respective templates for PCR, and PCR products were sequenced by second-generation sequencing technology. Crude mtDNA, mtDNAs isolated from crude mitochondria in HEK293T cells transfected with ssODN1 alone, mito-Cas9 system (sgRNA^{1ND4}-MTS^{COX8A}-Cas9-UTR^{SOD2} and ssODN1), with or without RS-1 treatment; purified mtDNA, mtDNAs isolated from crude mitochondria after DNase I digestion.

deletions were identified in the potential off-target sites of sgRNA^{1ND4} and sgRNA^{2ND4} (Table S2). We further screened the whole genome for GAATTC insertions using the WGS data. No nuclear DNA reads with the GAATTC insertion were detected, indicating that GAATTC knockin in the mtDNA reads of third-generation sequencing data was not caused by potential off-target and/or unspecific knockin in nuclear DNA or from NUMTs.⁷²

mtDNA pathogenic mutation generation using the mito-Cas9 system

Intragenic inversion mutation m.3902_3908inv (m.3902_3908 ACCTTGC>GCAAGGT) in the *MT-ND1* gene is reported to cause fatal infantile lactic acidosis and mitochondrial myopathy.^{73,74} At present, however, the underlying mechanism remains unclear. Here, using the same strategy, we designed the mito-Cas9 system to introduce the m.3902_3908inv mutation into HEK293T cells (Figure 5A). Successful knockin of ssODN³⁹⁰² in mtDNA within the mitochondria was demonstrated using a DNase protection assay (Figure 5B). Consistent with previous observations from the ssODN^{1ND4} and ssODN^{2ND4} knockin experiments, cells co-transfected with the mito-Cas9 constructs and ssODN³⁹⁰² showed a significant increase in m.3902_3908inv-specific PCR products compared with cells transfected with ssODN³⁹⁰² alone or with a combination of ssODN³⁹⁰² and MTS^{COX8A}-Cas9-UTR^{SOD2} (no sgRNA) (Figure 5C). In addition, mutation m.3902_3908inv was identified in the second-generation sequencing reads (Figure 5D). The knockin efficiency of mutation m.3902_3908inv was about 0.05% (2,432 reads successfully edited among 5,284,619 raw reads). These results suggest that the mito-Cas9 system may serve as a promising approach for targeted knockin in mtDNA and could be optimized as a workable way to establish cellular models for studying mtDNA pathogenic mutations.

DISCUSSION

Currently, whether mtDNA can be edited by CRISPR-Cas9 remains controversial.^{4,39,40} Due to the lack of NHEJ repair, mtDNA with DSBs degrades rapidly,²⁴ resulting in a reduction in mtDNA copy number, and thus mtDNA-edited products have not been directly detected in previous research.^{40–42} In this study, in addition to adding MTSs to Cas9,^{40–45} we optimized the mitochondria-targeted Cas9 system by adding the 3' UTR of the *SOD2* gene to the downstream region of the *Cas9* gene to facilitate efficient mitochondrial localization of Cas9 mRNA. We confirmed that the developed mito-Cas9 system transported Cas9 into the mitochondria (Figure 1C) and enabled mtDNA manipulation. Importantly, we developed a PCR-free third-generation sequencing technology that effectively avoids artifacts caused by PCR amplification (e.g.,

template switching artifacts) and verified the accurate knockin of exogenous ssODNs into mtDNA using the mito-Cas9 system (Figure 3). Another straightforward approach to confirm the effectiveness and efficiency of mitochondria-targeted CRISPR-Cas9 system can be engineered by introducing mtDNA-based drug resistance. Currently, we are attempting to establish a drug-resistant cell line with the mtDNA mutation m.2991T>C in the 16S rRNA of mtDNA, which could facilitate selection by chloramphenicol.⁷⁵

Previous studies have shown that homologous arms longer than 40 bp exhibit higher HR efficiency than shorter arms.^{37,59} Based on this observation, we designed the homologous arms of three ssODNs (ssODN1, ssODN2, and ssODN³⁹⁰²), which were all 45 bp in length. We also investigated the knockin efficiency of ssODN⁵⁰ with shorter arms (22 bp). Results showed that the knockin efficiency of ssODN⁵⁰ was significantly lower than that of ssODN1 (Figure S10). Thus, the knockin efficiency of ssODN may be affected by its length, and optimizing homologous arm length to balance the stability and mitochondrial transport efficiency of ssODN could be helpful for increasing the knockin efficiency of the mito-Cas9 system.

The mechanism that maintain mitochondrial genome stability remain elusive. Notably, for the two main DNA repair pathways, NHEJ cannot be detected in mitochondria and the existence of HR in mitochondria is controversial.^{55,56,58,76} Consistent with previous study,⁵⁸ we found that RAD51, a key nuclear factor of the HR repair pathway, was translocated into the mitochondria (Figure 4A) and its activation with agonist RS-1 enabled a 2- to 5-fold increase in knockin efficiency of ssODNs into mtDNA (Figure 4B). In addition, the effects of RAD51 activation appeared to be specific to cells transfected with the mito-Cas9 system (Figure 4, Table 1). These findings and third-generation sequencing results suggest that mtDNA can be affected by the HR pathway, and activation of the HR pathway by RAD51 stimulation may enhance CRISPR-Cas9-mediated knockin in mtDNA. One unresolved question is how ssODN is imported into mitochondria, which requires further research. Several studies have shown that DNA and RNA can be transported into mitochondria in animal cells and in plants,^{42,77–80} and our study provides further evidence that FAM-labeled sgRNA and ssODN1 can be transported into mitochondria (Figures 1E, S2, and S6A).

Enthusiasm for mtDNA editing stems from the clinical need for the treatment of mitochondrial diseases caused by pathogenic mtDNA mutations, most of which are in a heteroplasmic state. Both mito-ZFN^{13,15,17,21} and mito-TALEN^{18–20,22} are effective in altering the heteroplasmic level of mutant mtDNA.^{17–19,22} For homoplasmic mtDNA mutations, base editing^{26,32,33} and CRISPR-Cas9-mediated HR knockin can be used to edit mutant mtDNA. However, one of the key problems with mtDNA editing is that each cell may have hundreds to thousands of mtDNA copies and the editing of each copy is unlikely. Thus, employing mtDNA-editing technology to cure mitochondrial diseases caused by mtDNA mutations remains a considerable challenge. In our study, knockin efficiency of the mito-Cas9 system was rather low (0.03%–0.23%) compared with the recently developed DdCBE method (5%–50%).²⁶ We speculate that the low efficiency may be due to inefficient mitochondrial transport of the editing system and limited editing efficiency of the Cas9 protein to mtDNA. Therefore, mito-Cas9 system optimization, either by improving the mitochondrial transport efficiency such as mitochondrial RNA transport (although we did not achieve better mtDNA editing efficiency in cells overexpressing PNPASE, which can regulate RNA-import to mitochondria,⁸¹ compared with cells overexpressing RAD51 [data not shown]) or by using engineered Cas proteins with higher editing efficiency,⁸² is essential for the application of this mtDNA editing system. Furthermore, the knockin efficiency varied for different types of mutations, which may be due to different sequence features of the targeted region (i.e., GC% content) or different targeting efficiencies of the sgRNAs. Despite its limited editing efficiency, the mito-Cas9 system has the potential for wider scope of variant replacement and can introduce accurate knockin of target variants without changing other loci in the same editing window, thereby serving as an alternative strategy for manipulating mtDNA, especially considering recent findings that mitochondrial base editors may induce extensive off-target editing in the nuclear genome.^{34,35} In addition, inducing a small fraction of wild-type mtDNA using the mito-Cas9 system, then altering the heteroplasmic level of the wild-type mtDNA using mito-ZFN or mito-TALEN technology, offers a promising strategy for editing homoplasmic pathogenic mtDNA mutations.

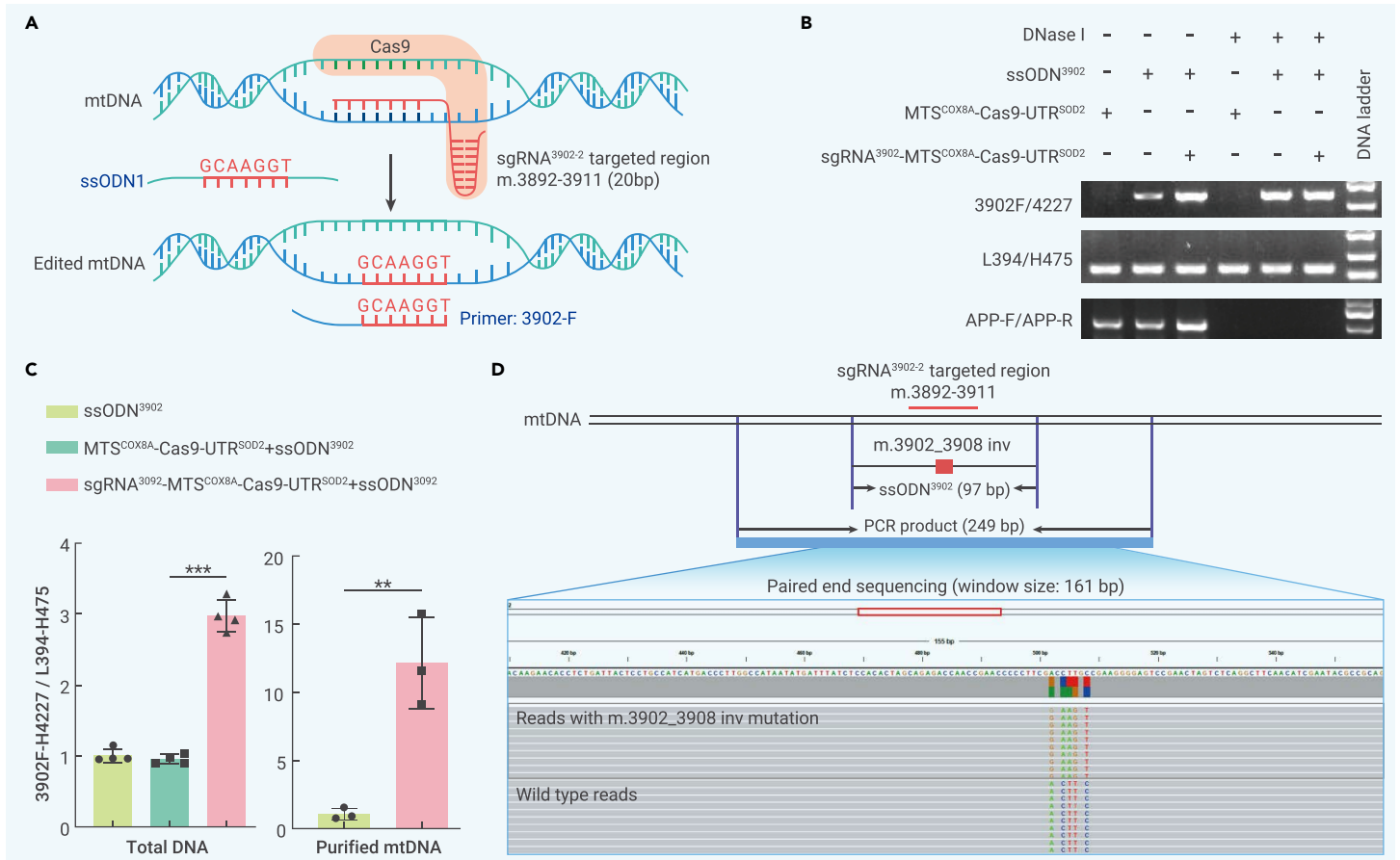


Figure 5. Introduction of pathogenic mutation m.3902_3908inv to mtDNA of HEK293T cells (A) Design of sgRNA and mito-Cas9-mediated knockin of mtDNA mutation m.3902_3908inv. (B) Site-specific PCR of mutation m.3902_3908inv. Crude mitochondria were extracted from HEK293T cells transfected with sgRNA³⁹⁰²⁻²-MTS^{COX8A}-Cas9-UTR^{SOD2} and ssODN³⁹⁰² for 48 h, then were treated with DNase I at 37°C for 1 h. PCR amplifications for nuclear *APP* (amplified by primer pair APP-F/APP-R), total mtDNA (amplified by primer pair L394/H475), and edited mtDNA (amplified by primer pair 3902F/H4227) were performed using the DNA template extracted from mitochondria with or without DNase I treatment. (C) Quantification of knockin efficiency of mutation m.3902_3908inv. HEK293T cells were transfected with or without a combination of Cas9 constructs and ssODN³⁹⁰². Proportion of mtDNA with successful m.3902_3908inv knockin (amplified by 3902F/H4227 (3902F-H4227)) was normalized to whole mtDNA (amplified by L394/H475 (L394-H475)). Bars are mean \pm SD. ns, not significant; **p < 0.01, ****p < 0.001. (D) Detection strategy and presence of m.3902_3908inv knockin in mtDNA reads generated by second-generation sequencing.

In conclusion, we established an mtDNA editing system based on CRISPR-Cas9-mediated knockin via the HR pathway and found that RAD51 agonist RS-1 significantly enhanced mtDNA knockin efficiency. Using PCR-free third-generation sequencing, we provide direct evidence for mtDNA editing mediated by the CRISPR-Cas9 system. Future studies devoted to increasing editing efficiency are essential for expanding the application and safety of the mito-Cas9 system in the treatment of mitochondrial diseases caused by pathogenic mtDNA mutations.

MATERIALS AND METHODS

Detailed materials and methods are included in the supplemental information.

DATA ACCESS

The data that support the findings of this work are available from the corresponding author upon reasonable request. The sequencing data were deposited at GSA (<https://ngdc.cnpc.ac.cn/gsa/>) under accession number HRA001435.

REFERENCES

- Schon, E.A., DiMauro, S., and Hirano, M. (2012). Human mitochondrial DNA: roles of inherited and somatic mutations. *Nat. Rev. Genet.* **13**, 878–890.
- Rahman, J., and Rahman, S. (2018). Mitochondrial medicine in the omics era. *Lancet* **391**, 2560–2574.
- Falkenberg, M., Larsson, N.G., and Gustafsson, C.M. (2007). DNA replication and transcription in mammalian mitochondria. *Annu. Rev. Biochem.* **76**, 679–699.
- Patananan, A.N., Wu, T.H., Chiou, P.Y., and Teitell, M.A. (2016). Modifying the mitochondrial genome. *Cell Metab.* **23**, 785–796.
- Yao, Y.G., Kajigaya, S., and Young, N.S. (2015). Mitochondrial DNA mutations in single human blood cells. *Mutat. Res.* **779**, 68–77.
- Russell, O., and Turnbull, D. (2014). Mitochondrial DNA disease-molecular insights and potential routes to a cure. *Exp. Cell Res.* **325**, 38–43.
- Taylor, R.W., and Turnbull, D.M. (2005). Mitochondrial DNA mutations in human disease. *Nat. Rev. Genet.* **6**, 389–402.
- Wallace, D.C., and Chalkia, D. (2013). Mitochondrial DNA genetics and the heteroplasmy conundrum in evolution and disease. *Cold Spring Harb. Perspect. Biol.* **5**, a021220.
- Ellouze, S., Augustin, S., Bouaita, A., et al. (2008). Optimized allotopic expression of the human mitochondrial ND4 prevents blindness in a rat model of mitochondrial dysfunction. *Am. J. Hum. Genet.* **83**, 373–387.
- Bi, R., Logan, I., and Yao, Y.G. (2017). Leber hereditary optic neuropathy: a mitochondrial disease unique in many ways. *Handb. Exp. Pharmacol.* **240**, 309–336.
- Herbert, M., and Turnbull, D. (2018). Progress in mitochondrial replacement therapies. *Nat. Rev. Mol. Cell Biol.* **19**, 71–72.
- Kang, E., Wu, J., Gutierrez, N.M., et al. (2016). Mitochondrial replacement in human oocytes carrying pathogenic mitochondrial DNA mutations. *Nature* **540**, 270–275.
- Minczuk, M., Papworth, M.A., Miller, J.C., et al. (2008). Development of a single-chain, quasi-dimeric zinc-finger nuclease for the selective degradation of mutated human mitochondrial DNA. *Nucleic Acids Res.* **36**, 3926–3938.
- Tanaka, M., Borgeld, H.J., Zhang, J., et al. (2002). Gene therapy for mitochondrial disease by delivering restriction endonuclease SmaI into mitochondria. *J. Biomed. Sci.* **9**, 534–541.
- Gammage, P.A., Viscomi, C., Simard, M.L., et al. (2018). Genome editing in mitochondria corrects a pathogenic mtDNA mutation in vivo. *Nat. Med.* **24**, 1691–1695.
- Bacman, S.R., Williams, S.L., Duan, D., and Moraes, C.T. (2012). Manipulation of mtDNA heteroplasmy in all striated muscles of newborn mice by AAV9-mediated delivery of a mitochondria-targeted restriction endonuclease. *Gene Ther.* **19**, 1101–1106.
- Gammage, P.A., Rorbach, J., Vincent, A.I., et al. (2014). Mitochondrially targeted ZFNs for selective degradation of pathogenic mitochondrial genomes bearing large-scale deletions or point mutations. *EMBO Mol. Med.* **6**, 458–466.
- Bacman, S.R., Kaupilla, J.H.K., Pereira, C.V., et al. (2018). MitoTALEN reduces mutant mtDNA load and restores tRNA(Ala) levels in a mouse model of heteroplasmic mtDNA mutation. *Nat. Med.* **24**, 1696–1700.

19. Pereira, C.V., Bacman, S.R., Arguello, T., et al. (2018). mitoTev-TALE: a monomeric DNA editing enzyme to reduce mutant mitochondrial DNA levels. *EMBO Mol. Med.* **10**, e8084.
20. Reddy, P., Ocampo, A., Suzuki, K., et al. (2015). Selective elimination of mitochondrial mutations in the germline by genome editing. *Cell* **161**, 459–469.
21. Minczuk, M., Papworth, M.A., Kolasinska, P., et al. (2006). Sequence-specific modification of mitochondrial DNA using a chimeric zinc finger methylase. *Proc. Natl. Acad. Sci. USA* **103**, 19689–19694.
22. Bacman, S.R., Williams, S.L., Pinto, M., et al. (2013). Specific elimination of mutant mitochondrial genomes in patient-derived cells by mitoTALENs. *Nat. Med.* **19**, 1111–1113.
23. Zekonyte, U., Bacman, S.R., Smith, J., et al. (2021). Mitochondrial targeted meganuclease as a platform to eliminate mutant mtDNA in vivo. *Nat. Commun.* **12**, 3210.
24. Peeva, V., Blei, D., Trombly, G., et al. (2018). Linear mitochondrial DNA is rapidly degraded by components of the replication machinery. *Nat. Commun.* **9**, 1727.
25. Moretton, A., Morel, F., Macao, B., et al. (2017). Selective mitochondrial DNA degradation following double-strand breaks. *PLoS One* **12**, e0176795.
26. Mok, B.Y., de Moraes, M.H., Zeng, J., et al. (2020). A bacterial cytidine deaminase toxin enables CRISPR-free mitochondrial base editing. *Nature* **583**, 631–637.
27. Lee, H., Lee, S., Baek, G., et al. (2021). Mitochondrial DNA editing in mice with DddA-TALE fusion deaminases. *Nat. Commun.* **12**, 1190.
28. Guo, J., Zhang, X., Chen, X., et al. (2021). Precision modeling of mitochondrial diseases in zebrafish via DdCBE-mediated mtDNA base editing. *Cell Discov.* **7**, 78.
29. Kang, B.C., Bae, S.J., Lee, S., et al. (2021). Chloroplast and mitochondrial DNA editing in plants. *Nat. Plants* **7**, 899–905.
30. Chen, X., Liang, D., Guo, J., et al. (2022). DdCBE-mediated mitochondrial base editing in human 3PN embryos. *Cell Discov.* **8**, 8.
31. Wei, Y., Xu, C., Feng, H., et al. (2022). Human cleaving embryos enable efficient mitochondrial base-editing with DdCBE. *Cell Discov.* **8**, 7.
32. Lim, K., Cho, S.I., and Kim, J.S. (2022). Nuclear and mitochondrial DNA editing in human cells with zinc finger deaminases. *Nat. Commun.* **13**, 366.
33. Cho, S.I., Lee, S., Mok, Y.G., et al. (2022). Targeted A-to-G base editing in human mitochondrial DNA with programmable deaminases. *Cell* **185**, 1764–1776.e12.
34. Wei, Y., Li, Z., Xu, K., et al. (2022). Mitochondrial base editor DdCBE causes substantial DNA off-target editing in nuclear genome of embryos. *Cell Discov.* **8**, 27.
35. Lei, Z., Meng, H., Liu, L., et al. (2022). Mitochondrial base editor induces substantial nuclear off-target mutations. *Nature* **606**, 804–811.
36. Hsu, P.D., Lander, E.S., and Zhang, F. (2014). Development and applications of CRISPR-Cas9 for genome engineering. *Cell* **157**, 1262–1278.
37. Ran, F.A., Hsu, P.D., Wright, J., et al. (2013). Genome engineering using the CRISPR-Cas9 system. *Nat. Protoc.* **8**, 2281–2308.
38. Gaj, T., Gersbach, C.A., and Barbas, C.F., 3rd (2013). ZFN, TALEN, and CRISPR/Cas-based methods for genome engineering. *Trends Biotechnol.* **31**, 397–405.
39. Gammage, P.A., Moraes, C.T., and Minczuk, M. (2018). Mitochondrial genome engineering: the revolution may not be CRISPR-ized. *Trends Genet.* **34**, 101–110.
40. Loutre, R., Heckel, A.M., Smirnova, A., et al. (2018). Can mitochondrial DNA be CRISPRized: Pro and Contra. *IUBMB Life* **70**, 1233–1239.
41. Jo, A., Ham, S., Lee, G.H., et al. (2015). Efficient mitochondrial genome editing by CRISPR/Cas9. *BioMed Res. Int.* **2015**, 305716.
42. Bian, W.P., Chen, Y.L., Luo, J.J., et al. (2019). Knock-in strategy for editing human and zebrafish mitochondrial DNA using mito-CRISPR/Cas9 system. *ACS Synth. Biol.* **8**, 621–632.
43. Antón, Z., Mullally, G., Ford, H.C., et al. (2020). Mitochondrial import, health and mtDNA copy number variability seen when using type II and type V CRISPR effectors. *J. Cell Sci.* **133**, jcs248468.
44. Wang, B., Lv, X., Wang, Y., et al. (2021). CRISPR/Cas9-mediated mutagenesis at microhomologous regions of human mitochondrial genome. *Sci. China Life Sci.* **64**, 1463–1472.
45. Hussain, S.R.A., Yalvac, M.E., Khoo, B., et al. (2021). Adapting CRISPR/Cas9 system for targeting mitochondrial genome. *Front. Genet.* **12**, 627050.
46. Hofreiter, M., Jaenicke, V., Serre, D., et al. (2001). DNA sequences from multiple amplifications reveal artifacts induced by cytosine deamination in ancient DNA. *Nucleic Acids Res.* **29**, 4793–4799.
47. Liu, S., Thaler, D.S., and Libchaber, A. (2002). Signal and noise in bridging PCR. *BMC Biotechnol.* **2**, 13.
48. Gilbert, M.T.P., Hansen, A.J., Willerslev, E., et al. (2003). Characterization of genetic miscoding lesions caused by postmortem damage. *Am. J. Hum. Genet.* **72**, 48–61.
49. Sylvestre, J., Margeot, A., Jacq, C., et al. (2003). The role of the 3' untranslated region in mRNA sorting to the vicinity of mitochondria is conserved from yeast to human cells. *Mol. Biol. Cell* **14**, 3848–3856.
50. Ginsberg, M.D., Felicelli, A., Jones, J.K., et al. (2003). PKA-dependent binding of mRNA to the mitochondrial AKAP121 protein. *J. Mol. Biol.* **327**, 885–897.
51. Gao, Z., Harwig, A., Berkhout, B., and Herrera-Carrillo, E. (2017). Mutation of nucleotides around the +1 position of type 3 polymerase III promoters: the effect on transcriptional activity and start site usage. *Transcription* **8**, 275–287.
52. Zhang, D., Zhang, H., Li, T., et al. (2017). Perfectly matched 20-nucleotide guide RNA sequences enable robust genome editing using high-fidelity SpCas9 nucleases. *Genome Biol.* **18**, 191.
53. He, T., Hatem, E., Vernis, L., et al. (2015). PRX1 knockdown potentiates vitamin K3 toxicity in cancer cells: a potential new therapeutic perspective for an old drug. *J. Exp. Clin. Cancer Res.* **34**, 152.
54. Feng, Y.M., Jia, Y.F., Su, L.Y., et al. (2013). Decreased mitochondrial DNA copy number in the hippocampus and peripheral blood during opiate addiction is mediated by autophagy and can be salvaged by melatonin. *Autophagy* **9**, 1395–1406.
55. Kajander, O.A., Karhunen, P.J., Holt, I.J., and Jacobs, H.T. (2001). Prominent mitochondrial DNA recombination intermediates in human heart muscle. *EMBO Rep.* **2**, 1007–1012.
56. D'Aurelio, M., Gajewski, C.D., Lin, M.T., et al. (2004). Heterologous mitochondrial DNA recombination in human cells. *Hum. Mol. Genet.* **13**, 3171–3179.
57. Tadi, S.K., Sebastian, R., Dahal, S., et al. (2016). Microhomology-mediated end joining is the principal mediator of double-strand break repair during mitochondrial DNA lesions. *Mol. Biol. Cell* **27**, 223–235.
58. Dahal, S., Dubey, S., and Raghavan, S.C. (2018). Homologous recombination-mediated repair of DNA double-strand breaks operates in mammalian mitochondria. *Cell. Mol. Life Sci.* **75**, 1641–1655.
59. Zhang, X., Li, T., Ou, J., et al. (2022). Homology-based repair induced by CRISPR-Cas nucleases in mammalian embryo genome editing. *Protein Cell* **13**, 316–335.
60. Qi, L.S., Larson, M.H., Gilbert, L.A., et al. (2013). Repurposing CRISPR as an RNA-guided platform for sequence-specific control of gene expression. *Cell* **152**, 1173–1183.
61. Shen, B., Zhang, W., Zhang, J., et al. (2014). Efficient genome modification by CRISPR-Cas9 nickase with minimal off-target effects. *Nat. Methods* **11**, 399–402.
62. Parr, R.L., Maki, J., Reguly, B., et al. (2006). The pseudo-mitochondrial genome influences mistakes in heteroplasmy interpretation. *BMC Genom.* **7**, 185.
63. Andrews, R.M., Kubacka, I., Chinnery, P.F., et al. (1999). Reanalysis and revision of the Cambridge reference sequence for human mitochondrial DNA. *Nat. Genet.* **23**, 147.
64. Tsuji, J., Frith, M.C., Tomii, K., and Horton, P. (2012). Mammalian NUMT insertion is non-random. *Nucleic Acids Res.* **40**, 9073–9088.
65. Ardui, S., Ameur, A., Vermeesch, J.R., and Hestand, M.S. (2018). Single molecule real-time (SMRT) sequencing comes of age: applications and utilities for medical diagnostics. *Nucleic Acids Res.* **46**, 2159–2168.
66. Sage, J.M., Gildemeister, O.S., and Knight, K.L. (2010). Discovery of a novel function for human Rad51: maintenance of the mitochondrial genome. *J. Biol. Chem.* **285**, 18984–18990.
67. Mishra, A., Saxena, S., Kaushal, A., and Nagaraju, G. (2018). RAD51C/XRCC3 facilitates mitochondrial DNA replication and maintains integrity of the mitochondrial genome. *Mol. Cell Biol.* **38**, e00489-17.
68. Song, J., Yang, D., Xu, J., et al. (2016). RS-1 enhances CRISPR/Cas9- and TALEN-mediated knock-in efficiency. *Nat. Commun.* **7**, 10548.
69. Pinder, J., Salsman, J., and Dellaire, G. (2015). Nuclear domain 'knock-in' screen for the evaluation and identification of small molecule enhancers of CRISPR-based genome editing. *Nucleic Acids Res.* **43**, 9379–9392.
70. Jayatilaka, K., Sheridan, S.D., Bold, T.D., et al. (2008). A chemical compound that stimulates the human homologous recombination protein RAD51. *Proc. Natl. Acad. Sci. USA* **105**, 15848–15853.
71. Budke, B., Logan, H.L., Kalin, J.H., et al. (2012). RI-1: a chemical inhibitor of RAD51 that disrupts homologous recombination in human cells. *Nucleic Acids Res.* **40**, 7347–7357.
72. Yao, Y.G., Kong, Q.P., Salas, A., and Bandelt, H.J. (2008). Pseudomitochondrial genome haunts disease studies. *J. Med. Genet.* **45**, 769–772.
73. Musumeci, O., Andreu, A.L., Shanske, S., et al. (2000). Intragenic inversion of mtDNA: a new type of pathogenic mutation in a patient with mitochondrial myopathy. *Am. J. Hum. Genet.* **66**, 1900–1904.
74. Blakely, E.L., Rennie, K.J., Jones, L., et al. (2006). Sporadic intragenic inversion of the mitochondrial DNA MTND1 gene causing fatal infantile lactic acidosis. *Pediatr. Res.* **59**, 440–444.
75. King, M.P., and Attardi, G. (1988). Injection of mitochondria into human cells leads to a rapid replacement of the endogenous mitochondrial DNA. *Cell* **52**, 811–819.
76. Hagström, E., Freyer, C., Battersby, B.J., et al. (2014). No recombination of mtDNA after heteroplasmy for 50 generations in the mouse maternal germline. *Nucleic Acids Res.* **42**, 1111–1116.
77. Koulintchenko, M., Temperley, R.J., Mason, P.A., et al. (2006). Natural competence of mammalian mitochondria allows the molecular investigation of mitochondrial gene expression. *Hum. Mol. Genet.* **15**, 143–154.
78. Tarasenko, T.A., Klimenko, E.S., Tarasenko, V.I., et al. (2021). Plant mitochondria import DNA via alternative membrane complexes involving various VDAC isoforms. *Mitochondrion* **60**, 43–58.
79. Liu, X., Wang, X., Li, J., et al. (2020). Identification of meccirRNAs and their roles in the mitochondrial entry of proteins. *Sci China Life Sci.* **63**, 1429–1449.
80. Boesch, P., Ibrahim, N., Dietrich, A., and Lightowers, R.N. (2010). Membrane association of mitochondrial DNA facilitates base excision repair in mammalian mitochondria. *Nucleic Acids Res.* **38**, 1478–1488.
81. Wang, G., Chen, H.W., Oktay, Y., et al. (2010). PNPase regulates RNA import into mitochondria. *Cell* **142**, 456–467.
82. Chen, Y., Hu, Y., Wang, X., et al. (2022). Synergistic engineering of CRISPR-Cas nucleases enables robust mammalian genome editing. *Innovation* **3**, 100264.

ACKNOWLEDGMENTS

We thank Prof. Ge Shan for helpful discussions, Dr. Christine Watts for language editing, and Dr. Jiankui Zhou for sharing the PST1374-Cas9 vector and pST1374-N-NLS-flag-linker-

Cas9-D10A vector with mutation p.H840A. This study was supported by the National Science and Technology Innovation 2030 Major Program (2021ZD0200900), the National Natural Science Foundation of China (U1702284 and 31970560), Yunnan Province (202003AD150009 and 2019FA027), the Strategic Priority Research Program (B) of the Chinese Academy of Sciences (CAS) (XDB32020200) and the Youth Innovation Promotion.

AUTHOR CONTRIBUTIONS

Y.-G.Y., R.B., X.H., H.Z., and P.Z. designed the study. R.B. and Y.L. constructed the mito-Cas9 system. M.X. performed third-generation sequencing and analyzed the data. Q.Z., B.X., and X.Z. extracted DNA and performed PCR analysis. D.-F.Z. and X.L. carried out secondary generation sequencing and analyzed the results. R.B. and G.M. performed flow cy-

tometry. Y.-G.Y., R.B., M.X., and Y.L. wrote the first draft of the paper. All authors contributed to and approved the final version of the manuscript.

DECLARATION OF INTERESTS

The authors declare no competing interests.

SUPPLEMENTAL INFORMATION

Supplemental information can be found online at <https://doi.org/10.1016/j.xinn.2022.100329>.

LEAD CONTACT WEBSITE

http://sourcedb.kiz.cas.cn/yw/zjrc/sc/200908/t20090825_2446617.html.



Optimize Your Process

Proven Solutions for Roots Pumping Stations

Your added value

- Roots pumps of the HiLobe and OktaLine series meet all the requirements of customers
- Magnetically coupled pumping stations available – hermetically tight and maintenance-free
- Pressure range from atmospheric pressure to high vacuum
- Fast evacuation due to high compression ratio
- Pumping station combinations specially adapted to your process available for many applications

Pfeiffer Vacuum
(Shanghai) Co., Ltd.
T +86 21 3393 3940
www.pfeiffer-vacuum.cn

PFEIFFER  **VACUUM**

Your Success. Our Passion.



Official WeChat Account

The Innovation, Volume 3

Supplemental Information

Direct evidence of CRISPR-Cas9-mediated mitochondrial genome editing

Rui Bi, Yu Li, Min Xu, Quanzhen Zheng, Deng-Feng Zhang, Xiao Li, Guolan Ma, Bolin Xiang, Xiaojia Zhu, Hui Zhao, Xingxu Huang, Ping Zheng, and Yong-Gang Yao

Online Supplemental Information

Materials and Methods

Construction of mitochondrial-targeting CRISPR/Cas9 system

In this study, mito-Cas9 was constructed using the px330-mCherry vector (Addgene plasmid #98750)¹. Briefly, the nuclear localization sequence (NLS) and 3×flag sequences at the N-terminus of SpCas9 in the px330-mCherry vector were replaced with the mitochondrial-targeting sequence (MTS) of mitochondrial genes (*COX8A*, *COX10*, or *SOD2*), and the NLS at the C-terminus of SpCas9 was replaced with the 3'-UTR of the *SOD2* gene using a ClonExpress® MultiS One Step Cloning Kit (Vazyme, C113) (Figure S1). Two sgRNAs targeting the *MT-ND4* gene, including sgRNA1^{ND4} targeting the mtDNA region 11 697-11 716 (m.11 697-11 716) and sgRNA2^{ND4} targeting m.11 851-11 868 (Table S1), were designed using the Breaking-Cas tool (<https://bioinfogp.cnb.csic.es/tools/breakingcas>)² and cloned into the mito-Cas9 constructs. Two ssODNs (ssODN1, relative to sgRNA1^{ND4}; ssODN2, relative to sgRNA2^{ND4}) were designed, with each having a 45 bp homologous arm flanking a 6 bp insertion of the *EcoRI* restriction site “GAATTC” (Table S1). The sgRNA targeting the nuclear *APP* gene (coding amyloid-beta precursor protein) (sgRNA^{APP}) was cloned to the px330-mCherry vector to obtain the nuclear targeting Cas9 construct sgRNA^{APP}-NLS-Cas9. All constructs were validated by sequencing. Overall, the mito-Cas9 system designed in this study contained three main elements: 1) MTS of a mitochondrial gene (*COX8A*, *COX10*, or *SOD2*) inserted at the N-terminus of *Cas9*; 2) 3'-UTR of *SOD2* inserted downstream of *Cas9*; and 3) sgRNA (sgRNA1^{ND4} or sgRNA2^{ND4}) targeting mtDNA. Constructs of MTS^{COX8A}-Cas9-UTR^{SOD2} (no sgRNA) and sgRNA1^{ND4}-MTS^{COX8A}-dCas9-UTR^{SOD2} (catalytically dead Cas9 (dCas9), SpCas9 with mutations p.D10A and p.H840A³) were used as controls (Figure S1). The dCas9 was sub-cloned from the pST1374-N-NLS-flag-linker-Cas9-D10A vector⁴ with mutation p.H840A that was provided by Dr. Jiankui Zhou.

In order to further demonstrate the feasibility of introducing the m.3902_3908inv mutation using the mito-Cas9 system, we designed sgRNA targeting to the m.3892_3918 region of the *MT-ND1* gene and a ssODN containing this pathogenic mutation (ssODN³⁹⁰²) using the same strategy (Table S1).

Cell culture, transfection, and sorting

The HEK293T cells were obtained from the Kunming Cell Bank, Kunming Institute of Zoology, and were cultured in Dulbecco's modified Eagle's medium (DMEM; Thermo Fisher) supplemented with 10% fetal bovine serum (FBS; Thermo Fisher) at 37 °C in 5% CO₂. Cells were seeded in a 6-well plate at a density of 5×10⁵ cells/well for 12 h before transfection. The mito-Cas9 constructs (2.5 μg each) were transfected with or without ssODN (50 pmol each) into cells using Lipofectamine 3000 (Thermo Fisher) according to the manufacturer's protocols. Co-transfection of 6-carboxyfluorescein (FAM)-labeled sgRNA1^{ND4}/ssODN1 and pDsRed2-mito vector (Clontech, which expresses mitochondrial targeting red fluorescent protein, mito-RFP) were performed using the same strategy. At 48 h after transfection, cells were harvested and analyzed using flow cytometry (BD, Influx, USA) at 610 nm to detect cells with successful transfection of the mito-Cas9 constructs or the pDsRed2-mito vector, and at 535 nm to detect cells with successful transfection of FAM-labeled sgRNA1^{ND4}/ssODN1.

Proteinase and DNase protection assays

Crude mitochondrial preparations were isolated using a Mitochondria Crude Isolation Kit (GMS10006, GENMED, China). For the proteinase protection assay, crude mitochondrial fraction (20 μg) was treated with 50 μg/mL proteinase K (Axygen) for 30 min on ice to remove proteins outside the mitochondria, followed by treatment with 1 mM phenylmethylsulfonyl fluoride (Sigma-Aldrich, P7626) to stop the proteinase K reaction and collect purified mitochondria.

For the DNase protection assay, crude mitochondrial fraction (20 μ g) was treated in 50 μ L of reaction buffer containing 0.5 U/ μ L DNase I (Takara) at 37 °C for 1 h to remove DNA molecules outside the mitochondria, with purified mtDNA then extracted using an AxyPrep Multisource Genomic DNA Miniprep Kit (Axygen). PCR amplifications of nuclear *APP* gene (amplified by primer pair APP-F/APP-R), total mtDNA (amplified by primer pair L11338/H11944), and edited mtDNA (amplified by primer pair L11338/*EcoRI*-R, or 3902F/H4227) were performed using the DNA template extracted from mitochondria before and after DNase I treatment, respectively. The PCR reactions were conducted in a total volume of 20 μ L containing 1 \times PCR buffer, 1 unit of LaTaq (TaKaRa), 175 μ mol/L of each dNTP, 0.2 μ mol/L of each primer (Table S1), and about 50 ng DNA template. The following PCR procedures were used: a pre-denaturation cycle at 94 °C for 5 min; 35 amplification cycles of 94 °C for 30 s, 55 °C for 30 s and 72 °C for 35 s; and a final extension cycle at 72 °C for 7 min.

Western blotting

Nuclear and cytoplasmic components from the HEK293T cells transfected with the mito-Cas9 constructs (2×10^6 cells for each construct) were extracted using a Nuclear and Cytoplasmic Protein Extraction Kit (Beyotime, P0027) following the manufacturer's instructions. For collection of total cell protein, the HEK293T cells were lysed in cell lysis buffer (Beyotime, China, P0013) and protein concentration was determined using a BCA Protein Assay Kit (Beyotime, P0012). Protein (20 μ g) was separated using 12% sodium dodecyl sulfate (SDS) polyacrylamide gel electrophoresis (PAGE) and transferred to a polyvinylidene difluoride membrane (Bio-Rad, 162-0177). After blocking with 5% (w/v) non-fat dry milk in Tris-buffered saline with 0.1% Tween 20 (TBST) for 2 h at room temperature, the membrane was incubated with respective primary monoclonal antibodies overnight at 4 °C. After three washes with TBST, the membrane was incubated with anti-mouse/rabbit IgG peroxidase-conjugated secondary antibodies (KPL), then the epitope was visualized using Immobilon Western Chemiluminescent HRP Substrate (Millipore, WBKLS0500). Primary antibodies included antibodies against Cas9 (Cell Signaling Technology, 14697T), Flag tag (Abmart, M20008L), ATP5A (Proteintech, 14676-1-AP), H3 (Cell Signaling Technology, 4499S), GAPDH (Proteintech, 60004-1-Ig), MFN2 (Proteintech, 12186-1-AP), COXIV (Cell Signaling Technology, 4850P), β -actin (Abmart, P30002F), RAD51 (Proteintech, 14961-1-AP) and α -tubulin (Enogene, E1C601). ImageJ (National Institutes of Health, Bethesda, MD) was used to quantify the protein expression level.

Quantification of mtDNA copy number and knock-in efficiency

Quantitative real-time PCR (qRT-PCR) was performed to measure the mtDNA copy number and knock-in efficiency of the mito-Cas9 system using the $2^{-\Delta\Delta CT}$ method, as described in our previous study⁵. In brief, mtDNA content was measured using primer pairs L394/H475 and L11718/H11944 (Table S1) and was normalized to a single-copy nuclear *β -globin* gene measured with primer pair HBB502f/HBB614r to determine the relative mtDNA copy number⁵. The proportion of mtDNA with successful knock-in of the *EcoRI* site "GAATTC" was measured using the *EcoRI* site-specific primer pair L11338/*EcoRI*-R (Table S1) and normalized to total mtDNA content measured using primer pair L394/H475. The ratio of mtDNA with the *EcoRI* site "GAATTC" relative to total mtDNA content was used to determine the knock-in efficiency of the mito-Cas9 system. A total of 20 ng of DNA was subjected to qRT-PCR using iTaq Universal SYBR Green Supermix (172-5125; Bio-Rad Laboratories) with the above indicated primer pairs on a CFX Connect Real-Time PCR Detection System (Bio-Rad Laboratories). The knock-in efficiency of ssODN2 and ssODN³⁹⁰² were determined with the same strategy (Table S1).

Examine the effect of RAD51 modulation on the knock-in efficiency mediated by mito-Cas9 system

We used RAD51 agonist⁶ RS-1 (Sigma, R9782) and inhibitor⁷ RI-1 (Merck Millipore, 553514) to activate and inhibit the RAD51 activity, respectively, and tested the potential

effect on the knock-in efficiency of the mito-Cas9 system. Briefly, RS-1 and RI-1 were dissolved in dimethyl sulfoxide (DMSO) at a concentration of 10 mM and 20 mM, respectively. After the HEK293T cells were transfected with the mito-Cas9 constructs for 6 h, the medium was changed with fresh growth medium supplemented with 10 μ M RS-1, 20 μ M RI-1, or an equal volume of DMSO (negative control). Cells were harvested for subsequent assays at 48 h post-transfection. We also evaluated the effect of RAD51 overexpression or knockdown on the knock-in efficiency of the mito-Cas9 system. The HEK293 cells were grown in 6-well plate for transfection of RAD51 overexpression vector (pcDNA3.1-RAD51, 1.25 μ g/well) (Public Protein/Plasmid Library) or control vector (pcDNA3.1, 1.25 μ g/well), together with mito-Cas9 construct sgRNA1^{ND4}-MTS^{COX8A}-Cas9-UTR^{SOD2} (1.25 μ g/well) and ssODN1 (50 pmol/well). For knockdown assay, control siRNA (siRNA^{NC}, 25 pmol/well) or siRNA targeting *RAD51* mRNA (siRNA^{RAD51}, 25 pmol/well) (Table S1) was co-transfected with mito-Cas9 construct sgRNA1^{ND4}-MTS^{COX8A}-Cas9-UTR^{SOD2} (2.5 μ g/well) and ssODN1 (50 pmol/well). Transfections were performed using Lipofectamine 3000 (Thermo Fisher) according to the manufacturer's protocols. Cells were harvested at 48 h after transfection for evaluating the knock-in efficiency.

Second-generation sequencing

We used second-generation sequencing technology (for mtDNA region m.11 600-11 820 amplified using mtDNA from HEK293T cells transfected with mito-Cas9) and third-generation sequencing technology (for mtDNA isolated from mitochondria and without PCR amplification) to identify edited mtDNA. For second-generation sequencing, purified mtDNA (mtDNA extracted from DNase I-treated mitochondria) and crude mtDNA (mtDNA extracted from crude mitochondria) from HEK293T cells transfected with or without a combination of the mito-Cas9 construct sgRNA1^{ND4}-MTS^{COX8A}-Cas9-UTR^{SOD2} and ssODN1 were used as templates for amplifying the mtDNA region m.11 600-11 820, which contained the potential knock-in of the *EcoRI* site (Table S1). The library was constructed using PCR products for paired-end sequencing on the Illumina NovaSeq platform. Raw reads were trimmed to remove sequencing adapters and low-quality reads using fastp v0.20.0⁸. The clean reads were aligned to the revised Cambridge reference sequence (rCRS, GenBank Accession No. NC_012920)⁹ using Burrows-Wheeler Aligner (BWA) v0.7.17-r1188¹⁰. Mapped reads <101 bp long were discarded to avoid potential noise from ssODNs (with a length of 96 bp), which might exist in the mtDNA extracts. Reads with the "GAATTC" insertion at the target region of sgRNA1^{ND4} were extracted using an in-house Perl script, which was available at the MitoTool (mitotool.kiz.ac.cn) web server (http://mitotool.kiz.ac.cn/lab/Extract_reads_with_GAATTC_insertion.pl). Sequence depth for each library was estimated using SAMtools v1.7¹¹. A fragment covering region m.3809-4058 was amplified and was subjected to second-generation sequencing using the same strategy to estimate the knock-in efficiency of ssODN³⁹⁰².

Third-generation sequencing

A total of 5×10^7 HEK293T cells were transfected with a combination of the mito-Cas9 construct sgRNA1^{ND4}-MTS^{COX8A}-Cas9-UTR^{SOD2} and ssODN1 for 48 h before harvesting to isolate crude mitochondria. We treated crude mitochondria with DNase I at 37 °C for 1 h to remove any DNA molecules outside the mitochondria, with the digested fraction then subjected to DNA extraction using an AxyPrep Multisource Genomic DNA Miniprep Kit (Axygen) to obtain purified mtDNA. Around 10 μ g of purified mtDNA was linearized by *BamHI* (100 U at 37 °C for 1 h, R0136S, New England Biolabs) at position m.14 258, followed by library construction based on the standard protocols for the Single-Molecule Real-Time (SMRT) long-read sequencing developed by Pacific Biosciences (PacBio). Purified mtDNA extracted from HEK293T cells transfected with a combination of the MTS^{COX8A}-Cas9-UTR^{SOD2} (no sgRNA) and ssODN1 was considered as control and was subjected to the same procedure for library construction. The library was sequenced on the PacBio Sequel II platform. In order to distinguish reads of nuclear DNA of mitochondrial origin (NUMT) from reads of mtDNA, we first generated circular consensus sequences (ccs)

from subreads using ccs v5.0.0 (<https://github.com/PacificBiosciences/ccs>). The ccs were then mapped to ± 30 kb region of all NUMTs reference sequences¹² and the extended version of rCRS⁹ with pbmm2 v1.3.0 (<https://github.com/PacificBiosciences/pbmm2>), respectively. The extended version of the reference sequence was composed of two complete rCRS sequences starting at the BamHI linearized site m.14 258. Ccs with MAPQ less than 30, mapped percentage (length mapped to reference sequence/total sequence length) less than 95%, and mapped concordance less than 95% were discarded. Subreads from ccs with higher mapped percentage and mapped concordance to NUMTs than to rCRS were considered as potential NUMTs. Subreads with a “GAATTC” insertion at the sgRNA1^{ND4} target region were extracted using an in-house Perl script (http://mitotool.kiz.ac.cn/lab/Extract_reads_with_GAATTC_insertion.pl) and were displayed using Integrative Genomics Viewer (IGV) v2.8.9.¹³

We also performed the third-generation sequencing using the Nanopore sequencing. Briefly, purified mtDNA extracted from HEK293T cells transfected with sgRNA1^{ND4}-MTS^{COX8A}-Cas9-UTR^{SOD2}+ssODN1 was sequenced using PromethION sequencing platform of Oxford Nanopore Technologies. Purified mtDNA extracted from HEK293T cells transfected with ssODN1 was used as a control. Libraries were prepared following the standard procedures. DNA fragments with length between 10000-20000 bp were selected by agarose gel to obtain relative intact mtDNA molecules. Sequencing reads with average quality score less than 15 were discarded. The remaining reads were mapped to the extended version of rCRS⁹ and ± 30 kb region of all NUMTs reference sequences¹² using minimap2 (<https://github.com/lh3/minimap2>)¹⁴, respectively. The mapped reads were analyzed using the same pipeline as described above. Because Nanopore has a relative higher sequencing error rate than PacBio¹⁵, we used a relative loose threshold for mapped concordance (80%) when analyzing the Nanopore data. For a read with “GAATTC” insertion, the quality of flanking sequence ± 10 bp of the insertion was estimated, and an average quality score less than 15 was discarded.

Off-target estimation

Genomic DNA was extracted from HEK293T cells grown in a 6-well plate that were transfected with sgRNA1^{ND4}-MTS^{COX8A}-Cas9-UTR^{SOD2}+ssODN1 and sgRNA2^{ND4}-MTS^{COX8A}-Cas9-UTR^{SOD2}+ssODN2, respectively. About 2 μ g genomic DNA per sample was used to prepare the whole-genome sequencing (WGS) library (150 bp paired-end), and sequenced on the DNBSEQ-T7 platform (Beijing Genomics institution, BGI). The quality of WGS data were checked by FastQC v0.11.9 (<http://www.bioinformatics.babraham.ac.uk/projects/fastqc>). Sequencing adapters and low-quality reads were removed by using the Trimmomatic v0.33¹⁶. The clean reads were then mapped to human reference genome GRCh38.p7 (hg38) using the Burrows-Wheeler Aligner¹⁰. Cas-Offinder¹⁷ was used to predict potential off-target sites of sgRNAs. Genomic sites with “NGG” or “NAG” PAM motifs and with up to nine mismatches with sgRNA1 or sgRNA2 were defined as potential off-target sites (Table S2). The predicted sites were subjected to CRISPRessoWGS of the CRISPResso2 software¹⁸ to explore the off-target events using the WGS data. Reads with low sequencing quality (quality <20) or mapping quality (MAPQ<60) were filtered from analysis. Frequencies of insertions, deletions, or substitutions within each potential off-target site in cells transfected with different sgRNAs were compared by *Fisher's* exact test to identify the potential off-target events.

Measurement of cellular reactive oxygen species (ROS) level and ATP level

The cellular ROS level and ATP level were determined using our previously described methods¹⁹. In brief, HEK293T cells transfected with different Cas9 constructs, including: 1) Cas9 (PST1374-Cas9 vector), expresses Cas9 protein without any targeting sequence²⁰; 2) NLS-Cas9: construct sgRNA^{APP}-NLS-Cas9 with removal of mcherry; 3) MTS-Cas9: construct sgRNA1^{ND4}-MTS^{COX8A}-Cas9-UTR^{SOD2} with removal of mcherry. After transfection for 24 h, cells were treated with vitamin K3 (vitK3; 7.5 μ M) or with melatonin (100 μ M) for another 24 h. Then, cells with and without treatment were harvested and incubated with

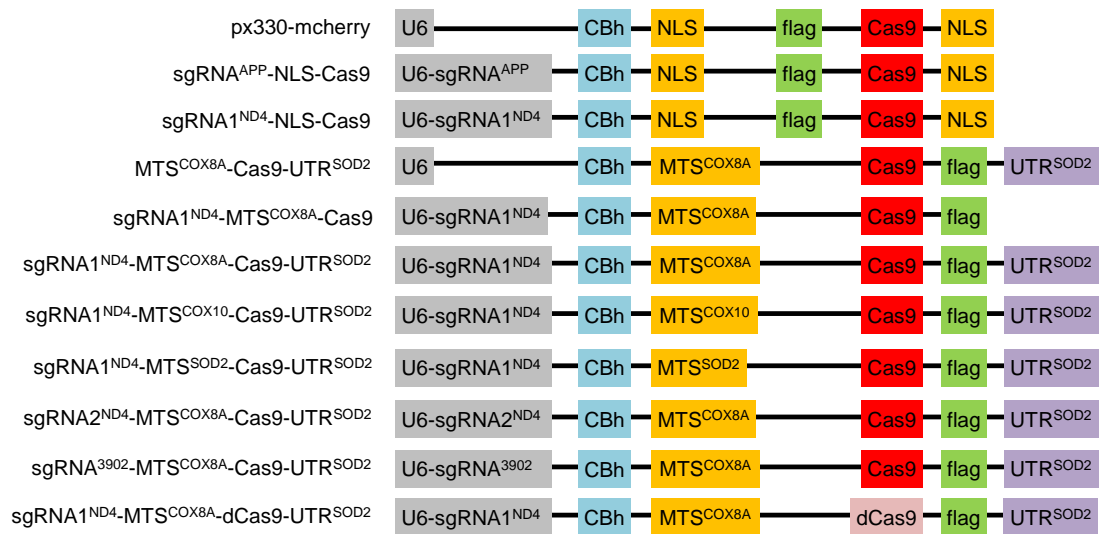
phosphate buffer saline (PBS) containing 0.5 μ M DCFH-DA probe (Sigma-Aldrich, D6883) at 37 °C for 20 min. Cells were washed with PBS and analyzed by using flow cytometry (BD, Vantage SE, USA) at 535 nm. For ATP measurement, cells seeded in 24-well plate were lysed in 100 μ L lysis buffer (GENMED, China, GMS10050). 10 μ L of cell lysate was subjected to ATP measurement according to the manufacture's manual for ATP Determination Kit (Invitrogen) on GloMax 96 Luminometer (Promega). The final ATP level was normalized by protein concentration of each sample.

Immunofluorescence assay

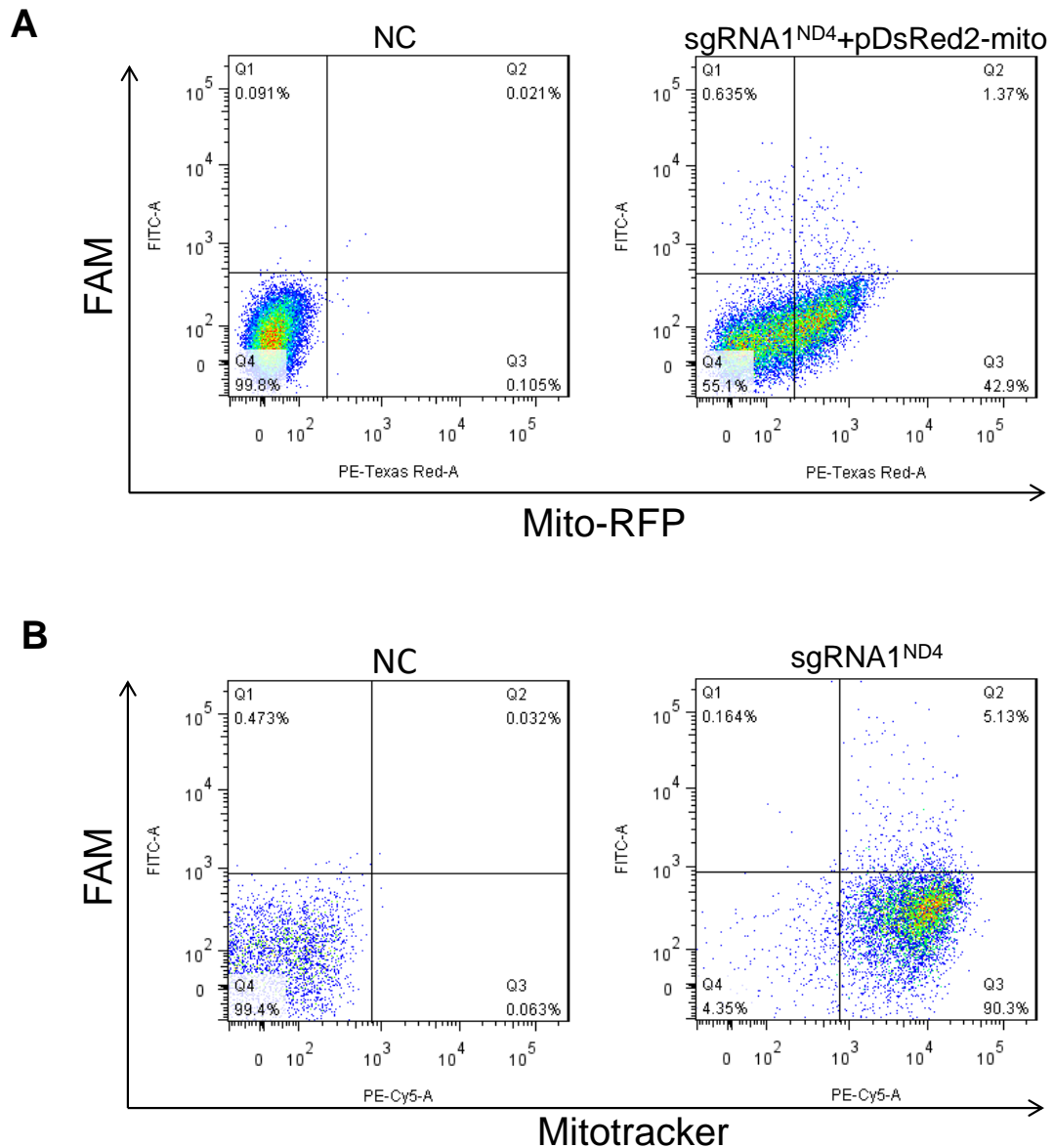
HEK293T cells were cultured on slides and were transfected with combinations of mito-GFP vector (expresses mitochondrial targeting green fluorescent protein (GFP)) and different Cas9 constructs (NLS-Cas9: construct sgRNA^{APP}-NLS-Cas9 with removal of mcherry; MTS-Cas9: construct sgRNA1^{ND4}-MTS^{COX8A}-Cas9-UTR^{SOD2} with removal of mcherry). Cells were fixed in 4 % paraformaldehyde for 30 min and were incubated with the Cas9 primary antibody (1:500, Cell Signaling Technology, 14697T) overnight at 4°C. After three washes with PBS (5 min each), cells were incubated with Alexa Fluor 594 -conjugated secondary antibody (1:500, ab150116, abcam) for 1 h at room temperature. Nuclear were stained by DAPI (1:1000; Invitrogen, D1306) for 15 min. The slides were visualized under an Olympus FluoView 1000 confocal microscope (Olympus).

Statistical analysis

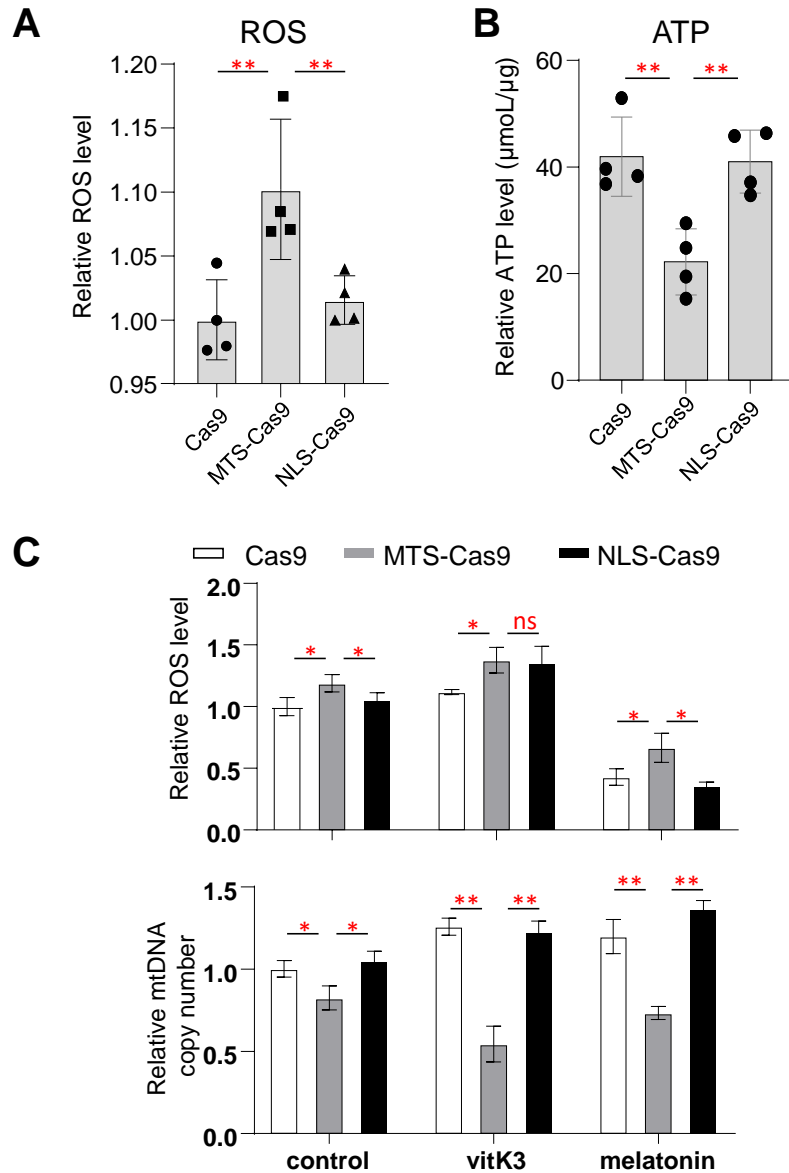
Differences in mtDNA copy number, ROS level, ATP level and knock-in efficiency among cells transfected with different constructs were quantified by two-tailed Student's *t*-test using GraphPad Prism software (GraphPad Software, La Jolla, CA, USA). Multiple comparisons were analyzed by one-way ANOVA test with adjustment of Tukey's multiple comparisons using GraphPad Prism software (GraphPad Software, La Jolla, CA, USA). $P < 0.05$ was considered statistically significant.



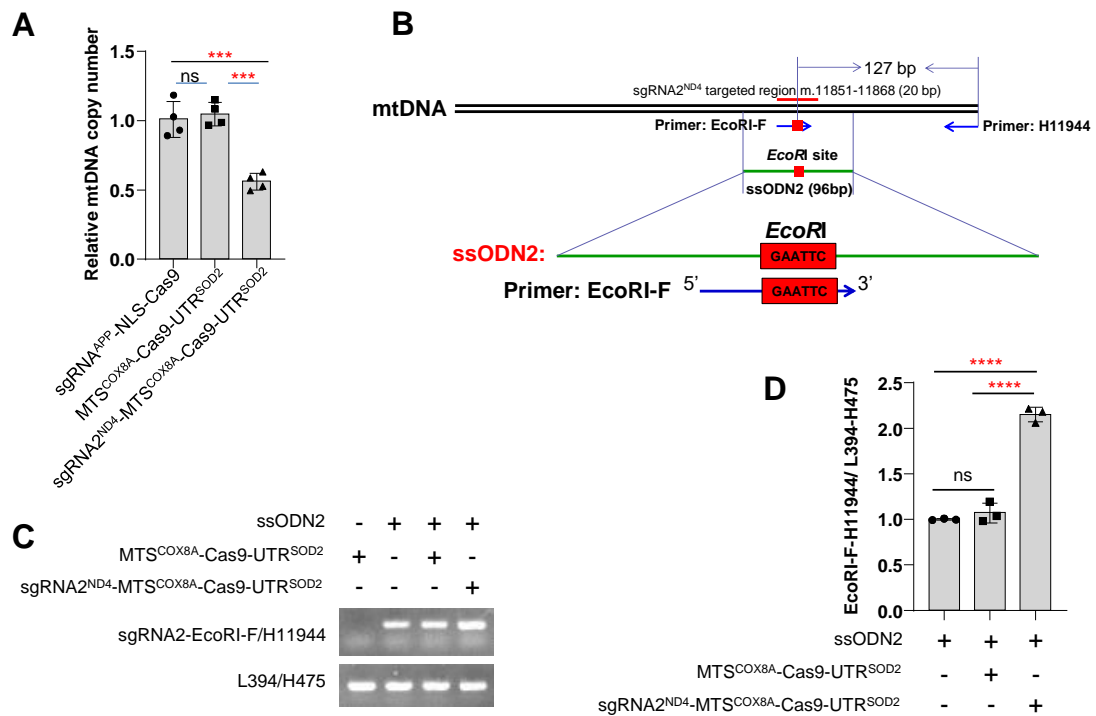
Supplementary Figure S1. Structure of the Cas9 constructs used in this study. The vector name was listed on the left of the schematic profile of each vector. UTR, 3'-untranslated region; MTS, mitochondrial-targeting sequence; NLS, nuclear localization sequence; CBh, chicken β -actin promoter; dCas9, catalytically dead Cas9, SpCas9 with mutations p.D10A and p.H840A^{3,4}. The two sgRNAs targeting to the *MT-ND4* gene are labeled as sgRNA1^{ND4} and sgRNA2^{ND4}, respectively. The sgRNA targeting to the nuclear *APP* gene and the sgRNA targeting m.3892-3918 region for introducing m.3902_3908inv (m.3902_3908 ACCTTGC>GCAAGGT) are labeled as sgRNA^{APP} and sgRNA³⁹⁰², respectively.



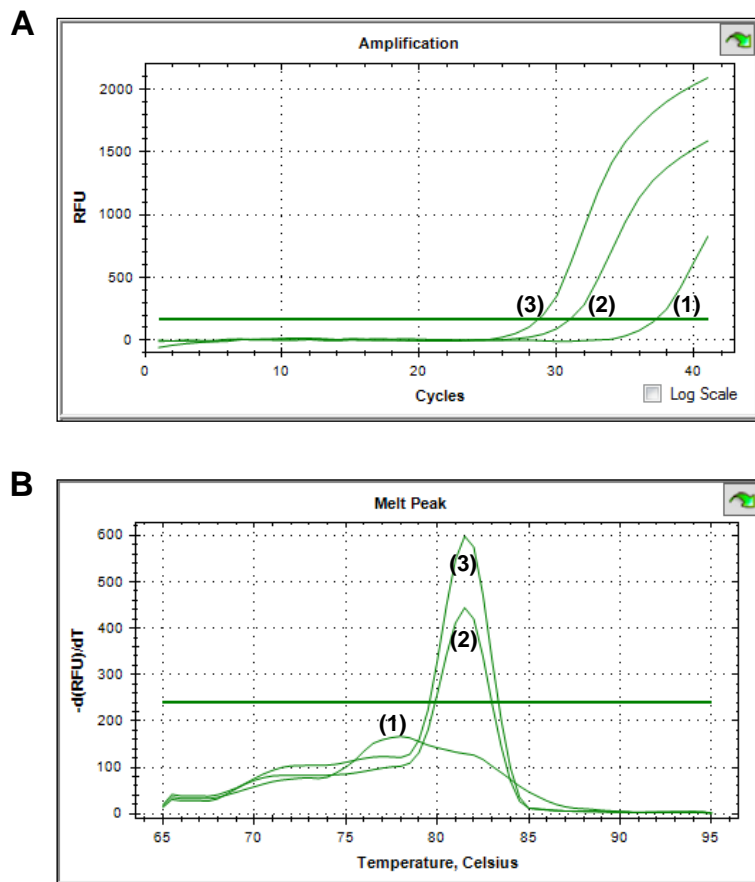
Supplementary Figure S2. Quantification of FAM-labeled sgRNA1^{ND4} in mitochondria using flow cytometry. (A) HEK293T cells were co-transfected with FAM-labeled sgRNA1^{ND4} and pDsRed2-mito vector (Clontech, expresses mitochondrial targeting red fluorescent protein, mito-RFP). Cells without any transfection were used as the negative control (NC). Crude mitochondria were isolated from cells at 48 h after transfection, and were subjected to flow cytometry. (B) HEK293T cells were transfected with FAM-labeled sgRNA1^{ND4} for 48h, then cells were incubated with 100 nM mitotracker (Molecular Probe, USA, M22425) for 30 min. Crude mitochondria were isolated from cells and were subjected to flow cytometry. Cells without any transfection and staining were used as the negative control (NC).



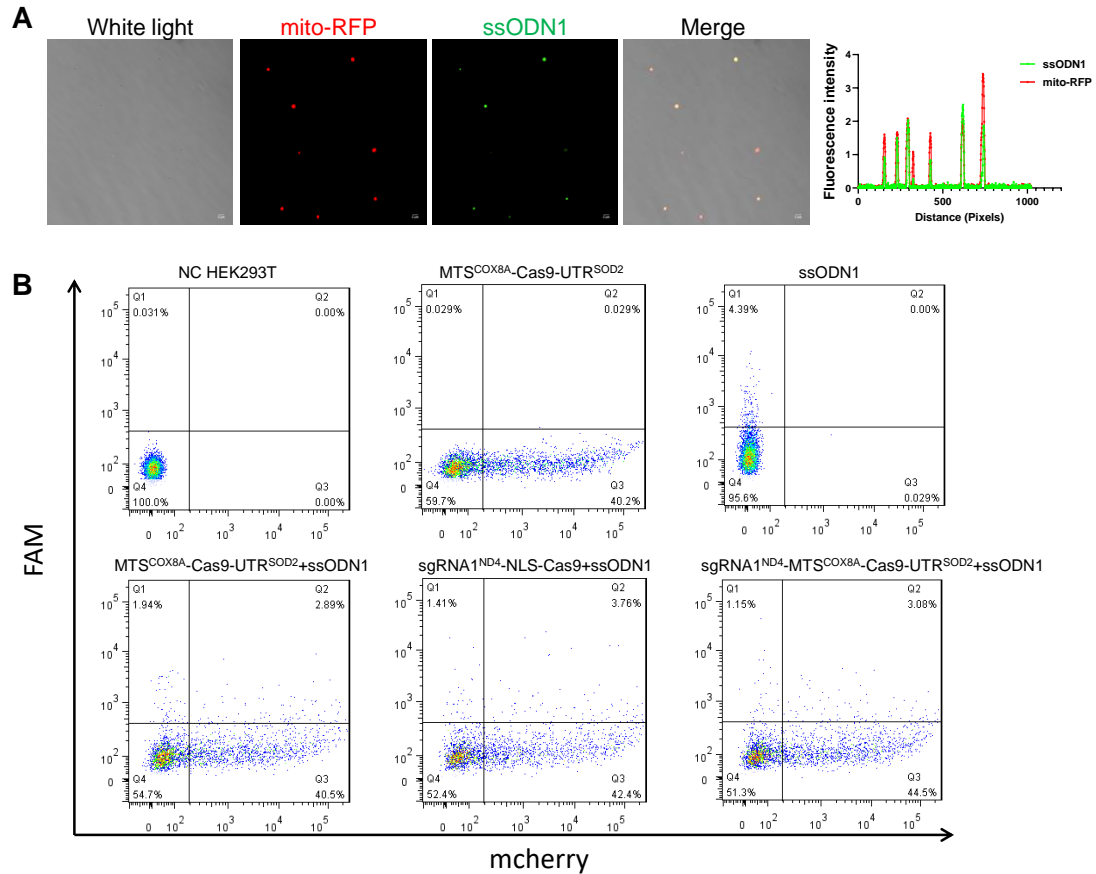
Supplementary Figure S3. Alterations of cellular reactive oxygen species (ROS) and ATP levels in cells transfected with the mito-Cas9 system. HEK293T cells were transfected with expression vector for Cas9 without any targeting sequence (Cas9), construct of Cas9 with mitochondrial targeting sequence (MTS-Cas9: construct sgRNA^{ND4}-MTS^{COX8A}-Cas9-UTR^{SOD2} with removal of mcherry), and construct of Cas9 with nuclear targeting sequence (NLS-Cas9: construct sgRNA^{APP}-NLS-Cas9 with removal of mcherry), respectively. **(A)** Cells were measured for the ROS levels at 48 h after transfection by using flow cytometry. **(B)** Measurement of the ATP levels in HEK293T cells after transfection for 48 h. **(C)** Measurement of cellular ROS levels and mtDNA copy number in transfected HEK293T cells with or without treatment of vitamin K3 (vitK3, 7.5 µM), melatonin (100 µM). Bars are mean ± SD. ns, not significant; *, $P < 0.05$; **, $P < 0.01$; one-way ANOVA test adjusted by Tukey's multiple comparisons tests.



Supplementary Figure S4. Editing of mtDNAs using the mito-Cas9 system with sgRNA2^{ND4}. (A) Quantification of mtDNA copy number for HEK293T cells transfected with nuclear-targeting Cas9 vector (sgRNA^{APP}-NLS-Cas9), mitochondrial-targeting Cas9 without sgRNA (MTS^{COX8A}-Cas9-UTR^{SOD2}) and mito-Cas9 construct (sgRNA2^{ND4}-MTS^{COX8A}-Cas9-UTR^{SOD2}). The mtDNA content was quantified by qRT-PCR with primer pair L394/H475, and was normalized to a single copy nuclear β -globin gene. (B) Design of the mito-Cas9 mediated knock-in system with sgRNA2^{ND4} and ssODN2. (C) *EcoRI* site-specific PCR with primer *EcoRI*-F/H11944. (D) Quantification of knock-in efficiency of ssODN2 by mito-Cas9 system using qRT-PCR. HEK293T cells were transfected with or without a combination of Cas9 constructs and ssODN2. Content of mtDNA with successful knock-in of *EcoRI* site (amplified by primer pair *EcoRI*-F/H11944) was normalized to whole mtDNA (total mtDNA, amplified by primer pair L394/H475). Bars are mean \pm SD. ns, not significant; ***, $P < 0.001$; ****, $P < 0.0001$; one-way ANOVA test adjusted by Tukey's multiple comparisons tests.

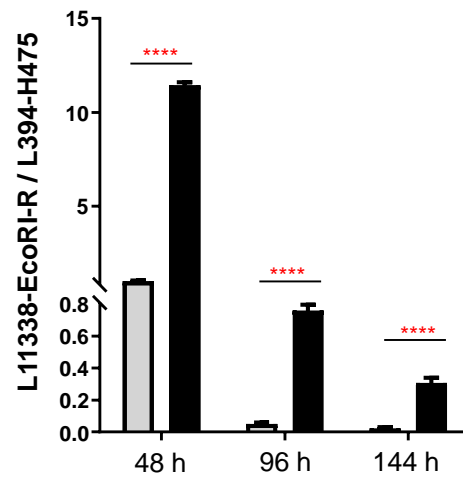


Supplementary Figure S5. Amplification curve (A) and melting curve (B) of the *EcoRI*-specific quantitative real-time PCR (qRT-PCR) products. The PCR products were amplified by using *EcoRI*-specific primer pair L11338/*EcoRI*-R with genomic DNA as the template. The genomic DNA samples were extracted from HEK293T cells with transfection of (1) MTS^{COX8A}-Cas9-UTR^{SOD2}, (2) ssODN1, (3) sgRNA1^{ND4}-MTS^{COX8A}-Cas9-UTR^{SOD2}+ssODN1, respectively, for 48 h.

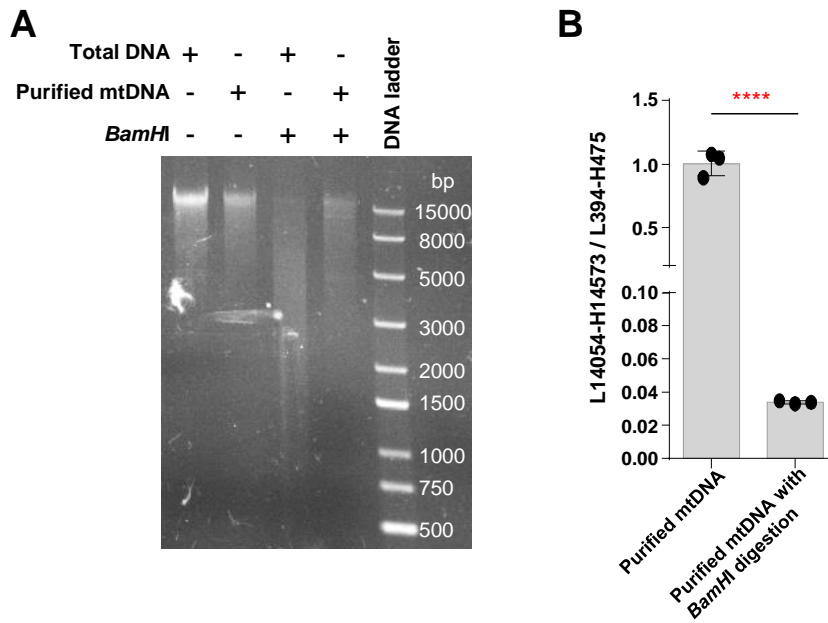


Supplementary Figure S6. Localization of the FAM-labeled ssODN1 in mitochondria and flow cytometry analyses of HEK293T cells with transfection of the FAM-labeled ssODN1 and/or Cas9 constructs. (A) Fluorescence microscopy assay of isolated mitochondria from HEK293T cells with transfection of the FAM-labeled ssODN1 and pDsRed2-mito vector (Clontech, expresses mitochondrial targeting red fluorescent protein, mito-RFP) for 48 h. (B) Flow cytometry analyses of the HEK293T cells transfected with or without the combination of FAM-labeled ssODN1 and different Cas9 constructs for 48 h. Cells were analyzed using flow cytometry (BD, Influx, USA) at 610 nm to detect mcherry that representing successful transfection of different Cas9 constructs, and at 535 nm to detect successful transfection of FAM-labeled ssODN1.

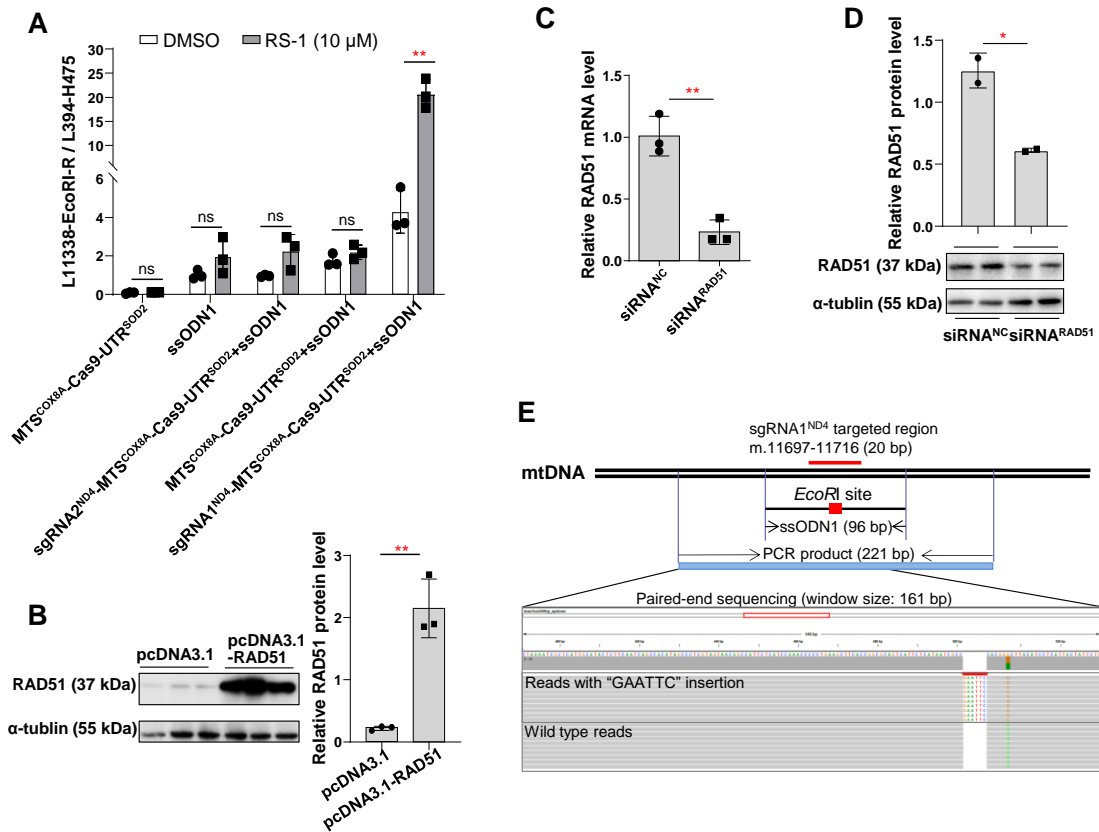
□ ssODN1
■ sgRNA1^{ND4}-MTS^{COX8A}-Cas9-UTR^{SOD2}+ssODN1



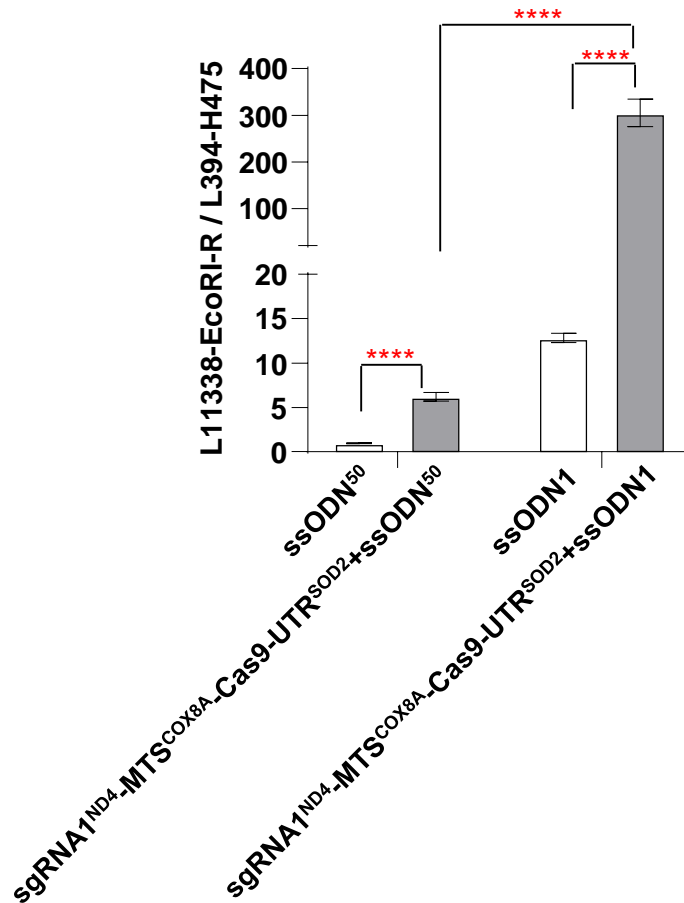
Supplementary Figure S7. Knock-in efficiency of the mito-Cas9 system in HEK293T cells. The HEK293T cells were transfected with ssODN1, with or without the mito-Cas9 system. The potential knock-in efficiency was quantified by qRT-PCR for transfected cells harvested at 48 h, 96 h and 144 h after transfection. Bars are mean \pm SD. ****, $P < 0.0001$; one-way ANOVA test adjusted by Tukey's multiple comparisons tests.



Supplementary Figure S8. Preparation of purified mtDNA for the third-generation sequencing. (A) Linearization of the mtDNA with *Bam*HI at site m.14258. Total DNA, total genomic DNA, including nuclear and mitochondrial DNA; Purified mtDNA, mtDNA extracted from DNase I treated crude mitochondria. The digestion was performed in a total volume of 100 μ L containing 10 μ g DNA and 100 unit of *Bam*HI at 37 $^{\circ}$ C for 3 h. (B) Quantification of non-linearized mtDNA molecules in purified mtDNAs with or without *Bam*HI digestion. qRT-PCR was performed using primer pair L14054/H14573 flanking the *Bam*HI site and primer pair L394/H475, to estimate the proportion of non-linearized mtDNA molecules. Linearized mtDNA could not be amplified by L14054/H14573. Bars are mean \pm SD. ****, $P < 0.0001$.



Supplementary Figure S9. Effects of RAD51 on the knock-in efficiency mediated by mito-Cas9 system. (A) Quantification of knock-in efficiency of different Cas9 groups with or without RAD51 activation. Four control groups were designed: 1) MTS^{COX8A}-Cas9-UTR^{SOD2}; 2) ssODN1 only; 3) sgRNA2^{ND4}-MTS^{COX8A}-Cas9-UTR^{SOD2}+ssODN1, sgRNA2^{ND4} targeting another region; 4) MTS^{COX8A}-Cas9-UTR^{SOD2}+ssODN1, mito-Cas9 without sgRNA. HEK293T cells were transfected with Cas9 construct or ssODN1, or with a combination of Cas9 construct and ssODN1 for 48 h. Purified mtDNA was extracted from Dnase I treated crude mitochondria from transfected HEK293T cells treated with DMSO or RS-1 (10 μM). Content of mtDNA with successful knock-in of *EcoRI* site (amplified by primer pair L11338/*EcoRI*-R) was normalized to whole mtDNA (amplified by primer pair L394/H475). (B) Overexpression of RAD51 in HEK293T cells. The HEK293T cells were co-transfected with pcDNA3.1-RAD51 or empty vector, together with mito-Cas9 construct and ssODN1. The RAD51 protein level was quantified and normalized to α -tubulin. (C-D) Knockdown of RAD51. HEK293T cells were transfected with control siRNA (siRNA^{NC}) or siRNA targeting *RAD51* mRNA (siRNA^{RAD51}), together with mito-Cas9 construct and ssODN1. The mRNA level of *RAD51* was quantified by qRT-PCR (C). The protein level of RAD51 was analyzed by Western blotting, and was normalized to α -tubulin (D). Bars are mean \pm SD. ns, not significant; *, $P < 0.05$; **, $P < 0.01$, one-way ANOVA test adjusted by Tukey's multiple comparisons tests in (A); two-tailed Student's *t* test in (B-D). (E) "GAATTC" insertions were identified in second-generation sequencing reads.



Supplementary Figure S10. The ssODN with long homologous arms (45 bp) had better knock-in efficiency than that with short homologous arms (22 bp). The HEK293T cells were transfected with ssODN1 (with a 45 bp homologous arm in each side) or ssODN⁵⁰ (with a 22 bp homologous arm in each side), together with or without the mito-Cas9 system. The knock-in efficiency was quantified by qRT-PCR for transfected cells after transfection for 48 h. Bars are mean \pm SD. ****, $P < 0.0001$; one-way ANOVA test adjusted by Tukey's multiple comparisons tests.

References

1. Wu, Y., Liang, D., Wang, Y., et al. (2013). Correction of a genetic disease in mouse via use of CRISPR-Cas9. *Cell Stem Cell* **13**, 659-662
2. Oliveros, J.C., Franch, M., Tabas-Madrid, D., et al. (2016). Breaking-Cas-interactive design of guide RNAs for CRISPR-Cas experiments for ENSEMBL genomes. *Nucleic Acids Res* **44**, W267-271
3. Qi, L.S., Larson, M.H., Gilbert, L.A., et al. (2013). Repurposing CRISPR as an RNA-guided platform for sequence-specific control of gene expression. *Cell* **152**, 1173-1183
4. Shen, B., Zhang, W., Zhang, J., et al. (2014). Efficient genome modification by CRISPR-Cas9 nickase with minimal off-target effects. *Nat Methods* **11**, 399-402
5. Bi, R., Zhang, A.M., Zhang, W., et al. (2010). The acquisition of an inheritable 50-bp deletion in the human mtDNA control region does not affect the mtDNA copy number in peripheral blood cells. *Hum Mutat* **31**, 538-543
6. Jayathilaka, K., Sheridan, S.D., Bold, T.D., et al. (2008). A chemical compound that stimulates the human homologous recombination protein RAD51. *Proc Natl Acad Sci U S A* **105**, 15848-15853
7. Budke, B., Logan, H.L., Kalin, J.H., et al. (2012). RI-1: a chemical inhibitor of RAD51 that disrupts homologous recombination in human cells. *Nucleic Acids Res* **40**, 7347-7357
8. Chen, S., Zhou, Y., Chen, Y., and Gu, J. (2018). fastp: an ultra-fast all-in-one FASTQ preprocessor. *Bioinformatics* **34**, i884-i890
9. Andrews, R.M., Kubacka, I., Chinnery, P.F., et al. (1999). Reanalysis and revision of the Cambridge reference sequence for human mitochondrial DNA. *Nat Genet* **23**, 147
10. Li, H., and Durbin, R. (2009). Fast and accurate short read alignment with Burrows-Wheeler transform. *Bioinformatics* **25**, 1754-1760
11. Li, H., Handsaker, B., Wysoker, A., et al. (2009). The Sequence Alignment/Map format and SAMtools. *Bioinformatics* **25**, 2078-2079
12. Tsuji, J., Frith, M.C., Tomii, K., and Horton, P. (2012). Mammalian NUMT insertion is non-random. *Nucleic Acids Res* **40**, 9073-9088
13. Robinson, J.T., Thorvaldsdottir, H., Winckler, W., et al. (2011). Integrative genomics viewer. *Nat Biotechnol* **29**, 24-26
14. Li, H. (2018). Minimap2: pairwise alignment for nucleotide sequences. *Bioinformatics* **34**, 3094-3100
15. Delahaye, C., and Nicolas, J. (2021). Sequencing DNA with nanopores: Troubles and biases. *PLoS One* **16**, e0257521
16. Bolger, A.M., Lohse, M., and Usadel, B. (2014). Trimmomatic: a flexible trimmer for Illumina sequence data. *Bioinformatics* **30**, 2114-2120
17. Bae, S., Park, J., and Kim, J.S. (2014). Cas-OFFinder: a fast and versatile algorithm that searches for potential off-target sites of Cas9 RNA-guided endonucleases. *Bioinformatics* **30**, 1473-1475
18. Clement, K., Rees, H., Canver, M.C., et al. (2019). CRISPResso2 provides accurate and rapid genome editing sequence analysis. *Nat Biotechnol* **37**, 224-226
19. Bi, R., Zhang, W., Yu, D., et al. (2015). Mitochondrial DNA haplogroup B5 confers

genetic susceptibility to Alzheimer's disease in Han Chinese. *Neurobiol Aging* **36**, 1604 e1607-1616

20. Shen, B., Zhang, J., Wu, H., et al. (2013). Generation of gene-modified mice via Cas9/RNA-mediated gene targeting. *Cell Res* **23**, 720-723